Table 4-13. Propionate:acetate ratios for source wells after different iniection strategies

Well	Sept. 2001 1X 6%	Oct. 2001 2 x 3%	Jan. 2002 2 x 3%	Mar. 2002 4X 6%	Jul. 2002 4 x 3%	Oct. 2002 4 x 3%
TSF-05A	1.16	1.06	1.12	1.24	0.95	1.04
TSF-05B	1.31	1.15	1.02	0.87	0.78	0.94
TAN-25	1.13	1.02	0.86	1.03	0.81	0.82
TAN-31	0.90	0.84	0.86	1.10	1.02	1.11

4.1.2 Redox Conditions

For ARD of chloroethenes to proceed to completion at meaningful rates, the process must be energetically favorable. The complete transformation of TCE to ethene by ARD requires the absence of the competing electron acceptors oxygen, nitrate, ferric iron, manganese (IV), and sulfate. In other words, for ARD of TCE to proceed to ethene, the redox conditions within the aquifer must be methanogenic. Methanogenic conditions are indicated by the absence of sulfate (and other acceptors), the presence of ferrous iron, and the presence of methane. Thus, the ferrous iron, sulfate, and methane concentrations were used to describe the redox conditions at locations throughout the treatment cell to determine whether the conditions for complete ARD have been created.

4.1.2.1 Source Area and Deep Wells. The source area and deep wells continued to be methanogenic throughout the reporting period; sulfate was completely absent, ferrous iron was elevated, and significant methane production was observed as concentrations approached the solubility limits in most wells (Figures 4-13 through 4-24). Decreases in methane concentrations below 5,000 µg/L following injections were likely due to dilution by the aerobic electron donor solution.

4.1.2.2 Downgradient Wells. Methane was present at all of the ISB downgradient monitoring locations. Methane at TAN-37A ranged from approximately 9,000 to 18,000 mg/L over the reporting period. Methane at TAN-37B rose sharply throughout the reporting period from 758 mg/L on November 19, 2002, to 22,294 mg/L on October 8, 2002. Methane at TAN-28 has fluctuated from a low value of 2,506 mg/L on September 10, 2001, to a high of 11,340 mg/L on September 9, 2002. In general, methane concentrations throughout the reporting period have been between 3,000 and 5,000 mg/L at TAN-28. TAN-30A methane concentrations have remained steady at approximately 10,000 mg/L. However, the presence of methane at the downgradient wells can be attributed to transport from the source area wells rather than to active methanogenesis. The evidence for this can be seen by assessing the sulfate and ferrous iron data from these wells.

As described in the previous section, the downgradient wells were rarely impacted by electron donor. TAN-37A and TAN-37B were impacted slightly following the March 25,2002, 4X 6% injection. Ferrous iron increased at TAN-37A from 0.03 mg/L on April 3, 2002 to 0.26 mg/L on April 17, 2002. At the same time, sulfate also dropped from 36 to 24 mg/L. However, by June 4, 2002, ferrous iron and sulfate had returned to their pre-4X 6% injection levels. TAN-37B was impacted in a similar manner as TAN-37A, with ferrous iron increasing from 0.04 mg/L on March 6, 2002, to 0.80 mg/L on April 3, 2002. At the same time, sulfate dropped from 35 mg/L on April 3, 2002, to 23 mg/L on April 17, 2002. As was the case with TAN-37A, by June 4, 2002, ferrous iron and sulfate had returned to the pre-4X 6% injection levels (33 mg/L).

4.1.2.3 Outside Wells. As described in Section 4.1.1, electron donor was not distributed to the outside well locations with one exception, TAN-D2. Therefore, as expected, methanogenic conditions

have only been created at TAN-D2. Electron donor was distributed to TAN-D2 following the March 25, 2002, 4X 6% injection. This electron donor did impact redox conditions; sulfate was 0 mg/L on April 2,2002, and ferrous iron was 3.00 mg/L, the upper limit of the analytical method. The presence of high concentrations of ferrous iron at TAN-D2 prior to the March 25, 2002, injection indicate that TAN-D2 has been on the edge of the donor-impacted zone since Summer 1999. Sulfate rebounded at this well by April 30, 2002, to 25 mg/L, but was depleted at this well again following the July 30, 2002, injection. This depletion of sulfate, coupled with the presence of methane, indicated that methanogenesis was probably occurring in TAN-D2. There was a slight rebound in sulfate to 9 mg/L on September 9, 2002, but conditions returned to methanogenic by October 7, 2002. None of the other outside wells was methanogenic.

4.1.3 Anaerobic Reductive Dechlorination

The efficiency of the ARD reactions is assessed using the relative molar concentrations of TCE, cis-DCE, vinyl chloride (VC), and ethene. High concentrations of ethene relative to TCE, cis-DCE, and VC indicate that ARD reactions are operating efficiently. Results are presented in Figures 4-25 through 4-38.

4.1.3.1 Source Wells. Anaerobic reductive dechlorination has continued in all source area wells throughout the reporting period. Ethene was the dominant compound at both TSF-05A and TSF-05B. TCE was observed to increase following each sodium lactate injection; however, concentrations were near or below the detection limit by the next sampling event (4 weeks later). VOCs spiked at TSF-05A and TSF-05B following the March 4X 6% injection. TCE at TSF-05A was 1,296 µg/L on April 1, 2002, 7 days after the injection. This TCE concentration was the second highest observed at this location since sampling began on October 12, 1999. On April 30, 2002 (5 weeks after injection), TCE was below the detection limit. Ethene at TSF-05A was lower immediately following the injection (7 days later), but had increased to 890 µg/L within 5 weeks of the injection. Throughout the reporting period, ethene continued to be the dominant compound at this location. A similar pattern occurred at TSF-05B with VOC concentrations increasing immediately following the injection. TCE at this location was 1,136 µg/L following the injection, the highest observed since sampling began on October 12, 1999. On May 1,2002, TCE was below detection limit. Ethene remained the dominant compound present at this location.

At TAN-25 and TAN-31, TCE remained near the detection limit. The molar ratio of cis-DCE relative to the total VOC concentration has increased since the onset of the 4X injection strategy in March 2002. Following the March 4X 6% injection, cis-DCE spiked sharply at both TAN-25 and TAN-31. Five weeks following injection, cis-DCE at TAN-31 was below detection, while the cis-DCE concentration at TAN-25 remained constant. However, cis-DCE continued to represent a high percentage of VOCs at both locations. Ethene at both locations was lower following the March 4X 6% injection than observed before the injection, and has continued to drop since that time. Trans-DCE continued to be a relatively recalcitrant compound at each of the source area wells. This is discussed further in Section 5.4.

Deep Wells — Volatile organic compounds in TAN-26 (with the exception of trans-DCE) have been near or below MCLs since January 2000 (Figure 4-29). VOCs in TAN-37C have been near or below MCLs since July 2000 (with the exception of trans-DCE). Trans-DCE has ranged from 80 to 130 µg/L in this well (Figure 4-30). Occasional spikes have been observed at both locations; however, these are sporadic and likely related to transient hydraulic conditions rather than a trend.

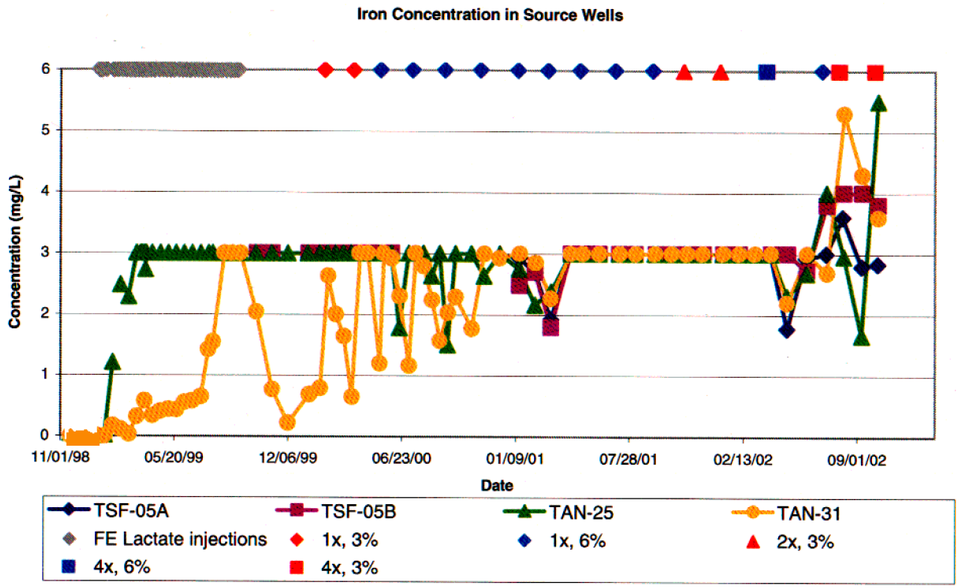

Figure 4-13. Source wells ferrous iron.

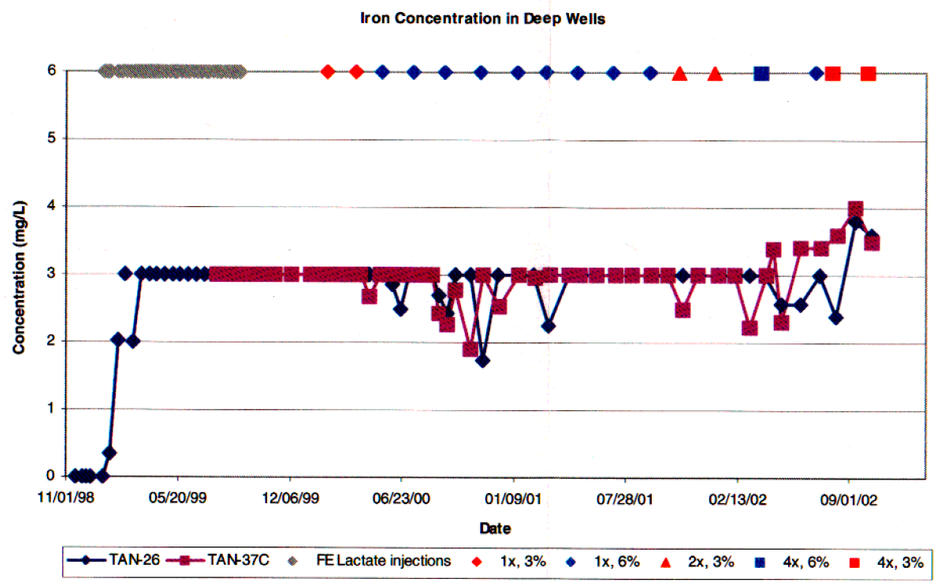

Figure 4-14. Deep wells ferrous iron.

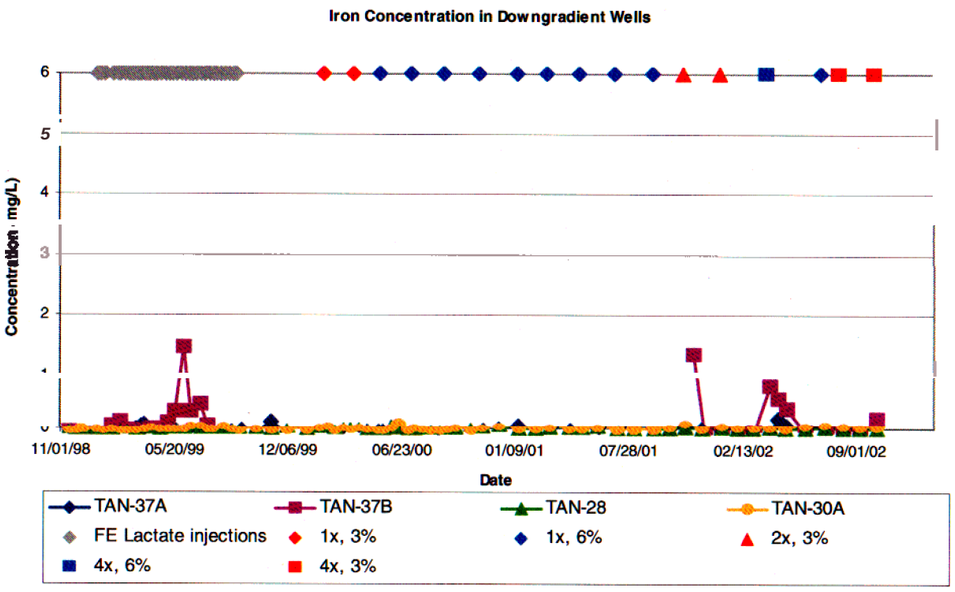

Figure 4-15. Downgradient wells ferrous iron.

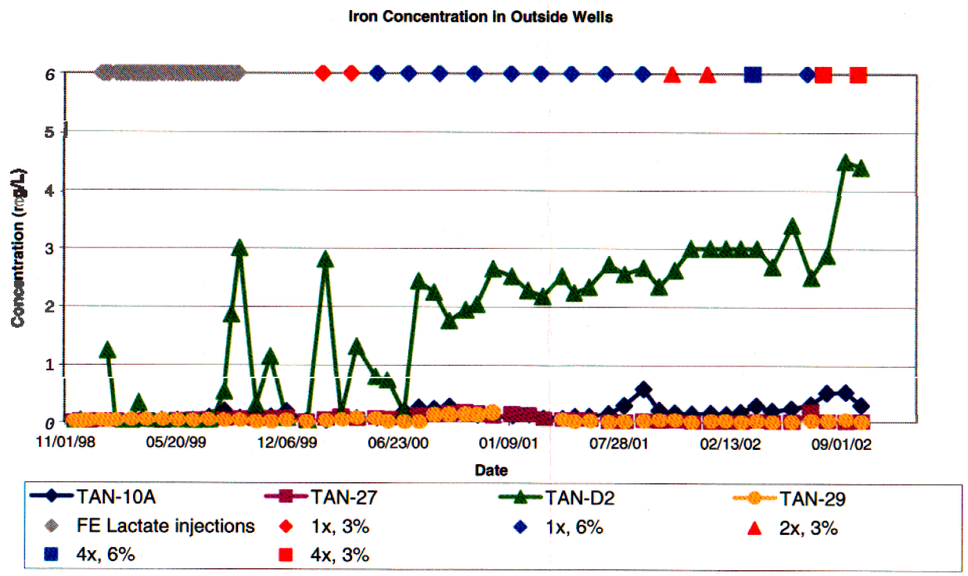

Figure 4-16. Outside wells ferrous iron.

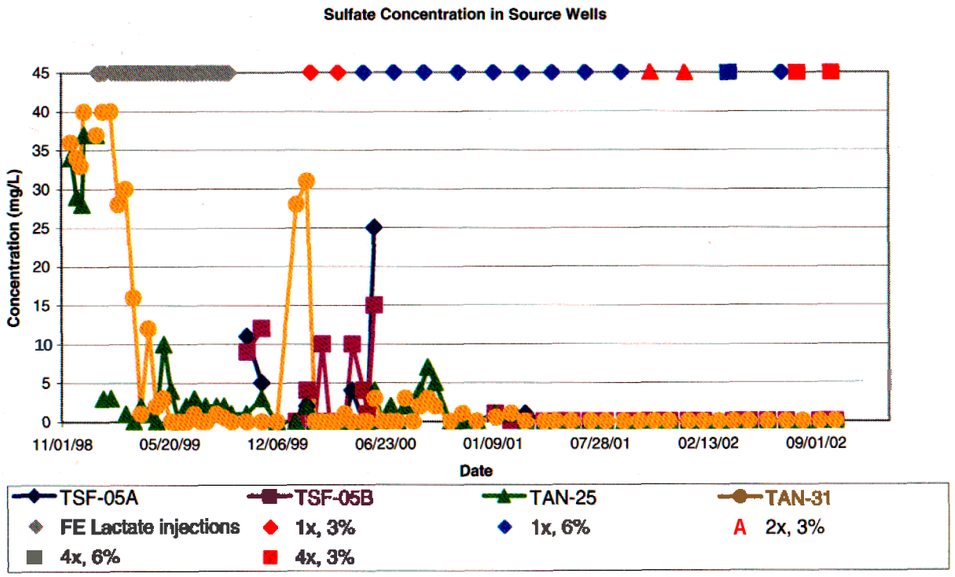

Figure 4-17. Source wells sulfate.

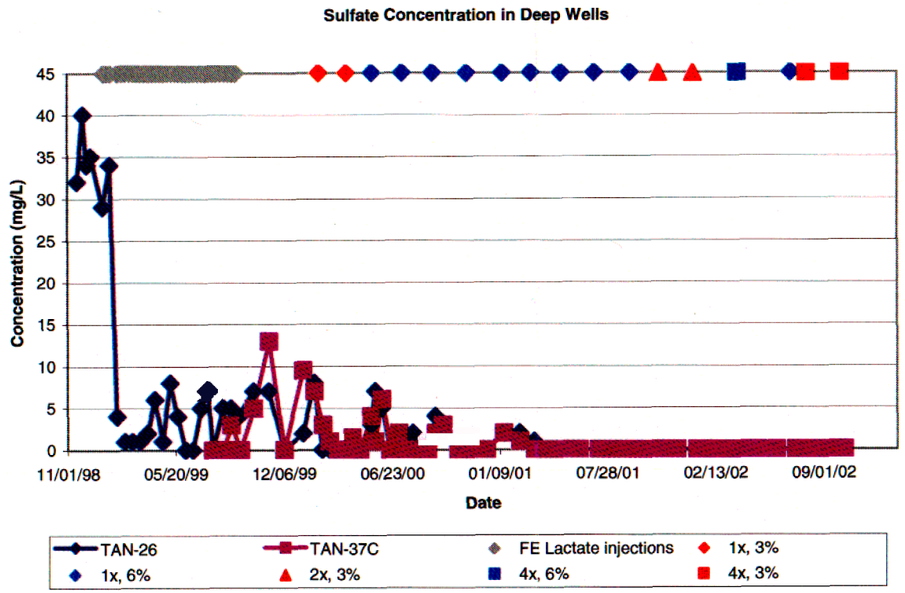

Figure 4-18. Deep wells sulfate.

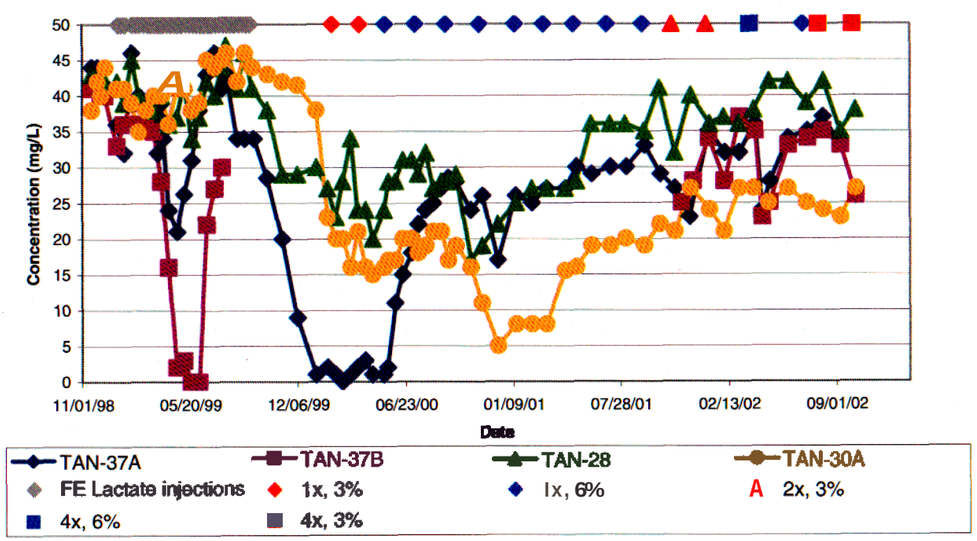

Figure 4-19. Downgradient wells sulfate.

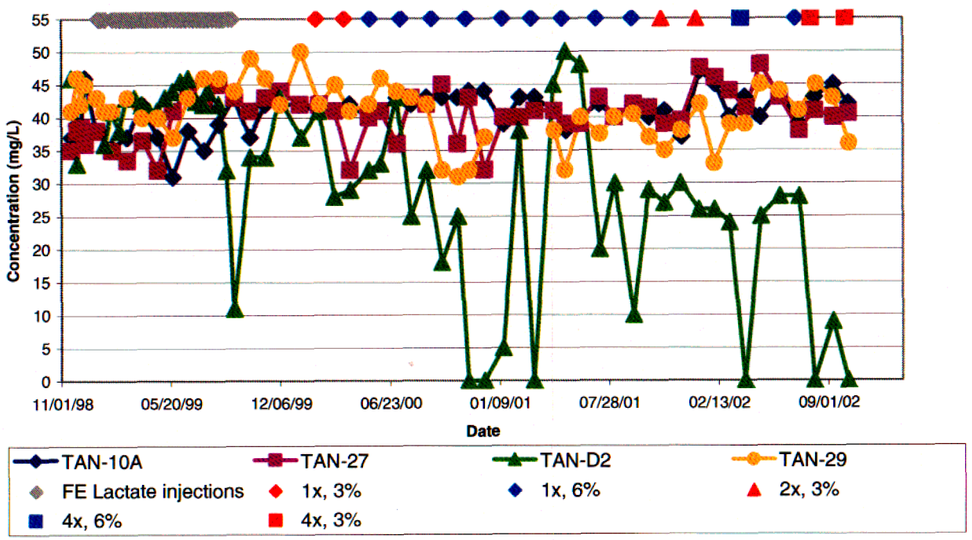

Figure 4-20. Outside wells sulfate.

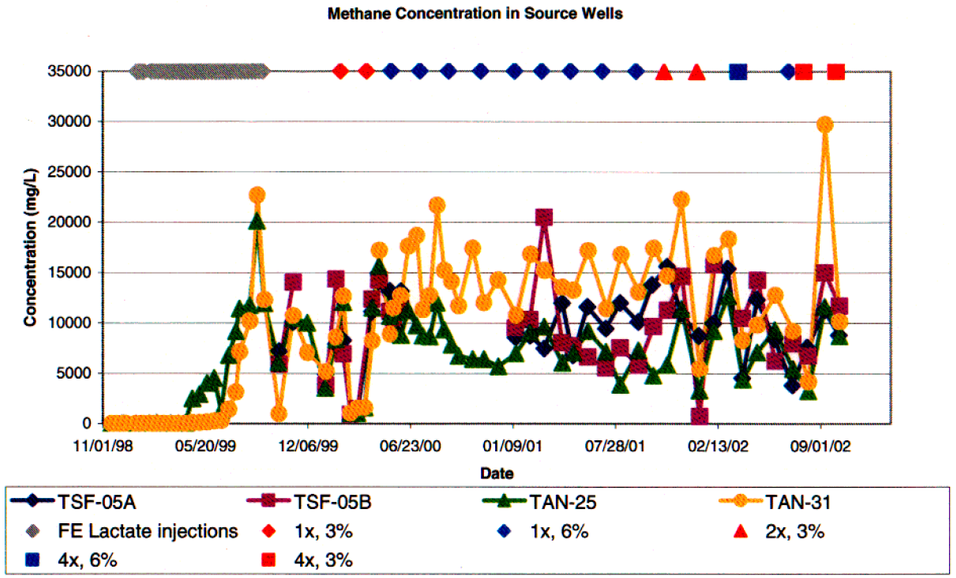

Figure 4-21. Source wells methane.

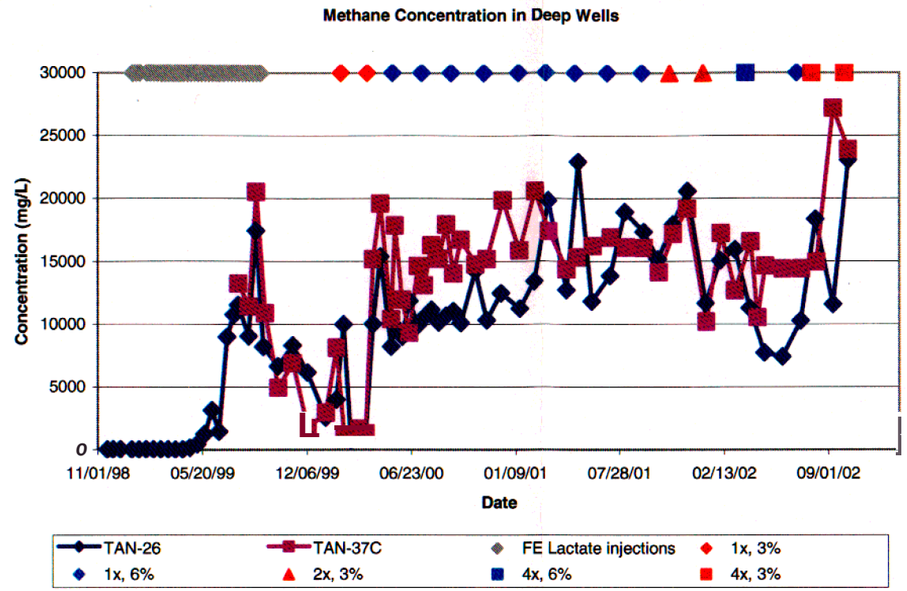

Figure 4-22. Deep wells methane.

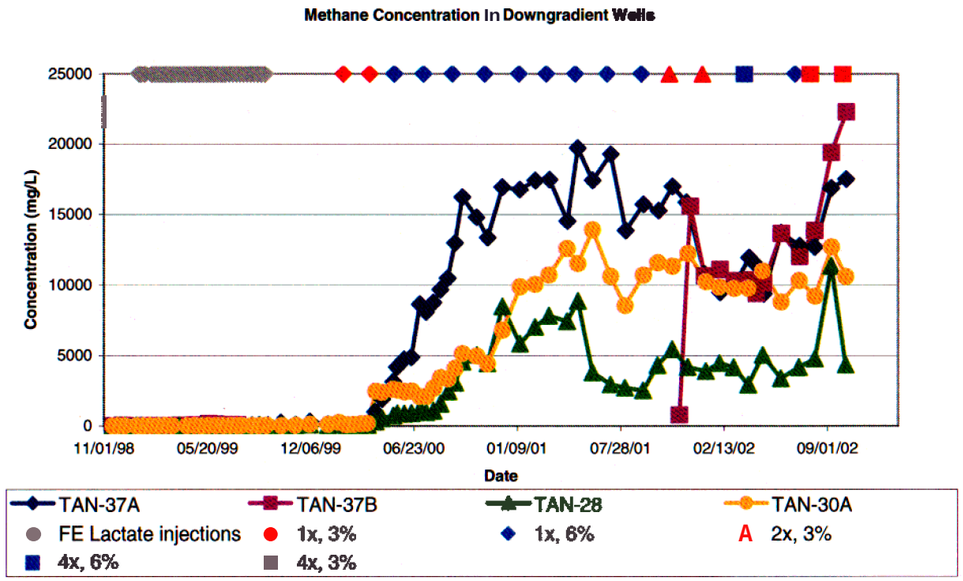

Figure 4-23. Downgradient wells methane.

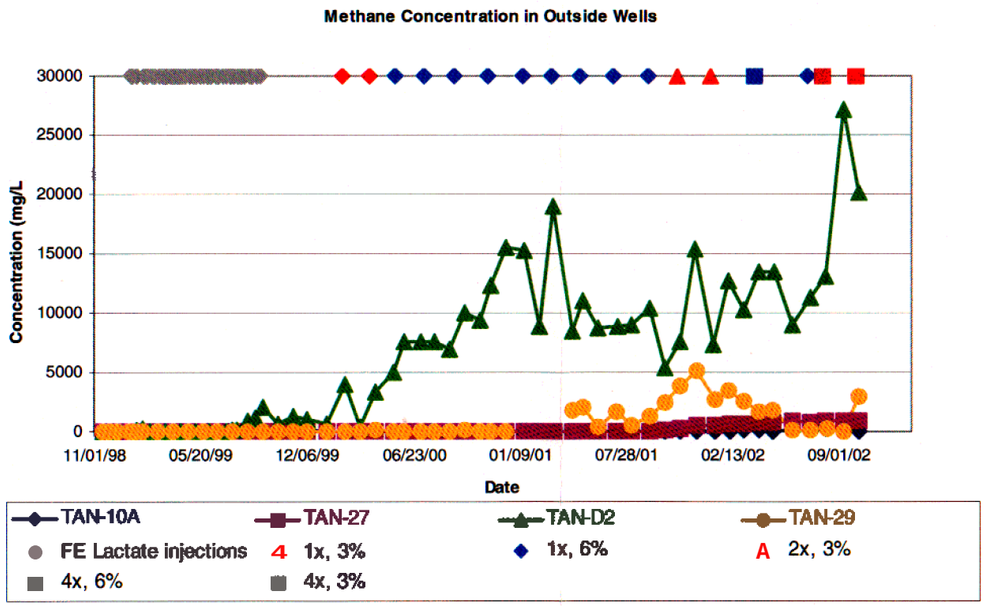

Figure 4-24. Outside wells methane.

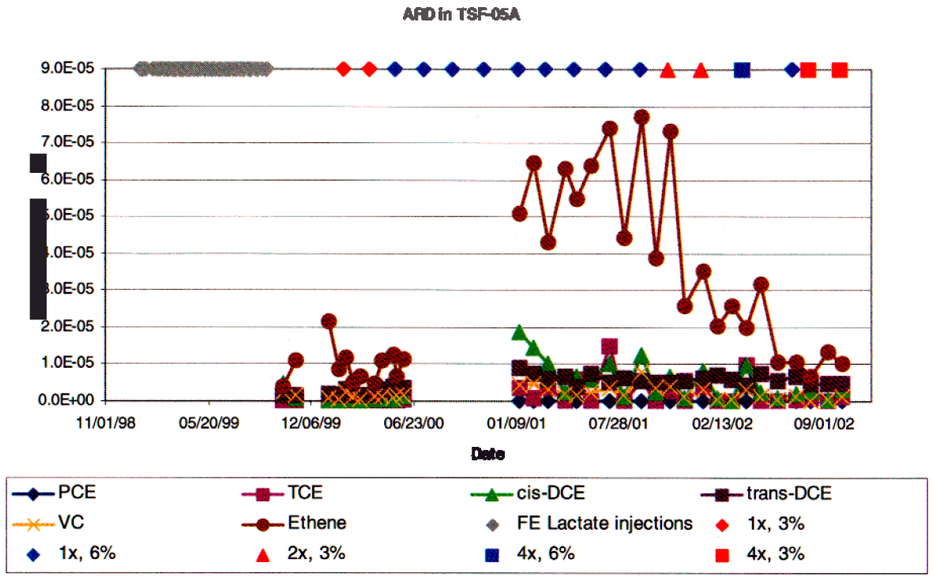

Figure 4-25. Anaerobic reductive dechlorination in TSF-05A.

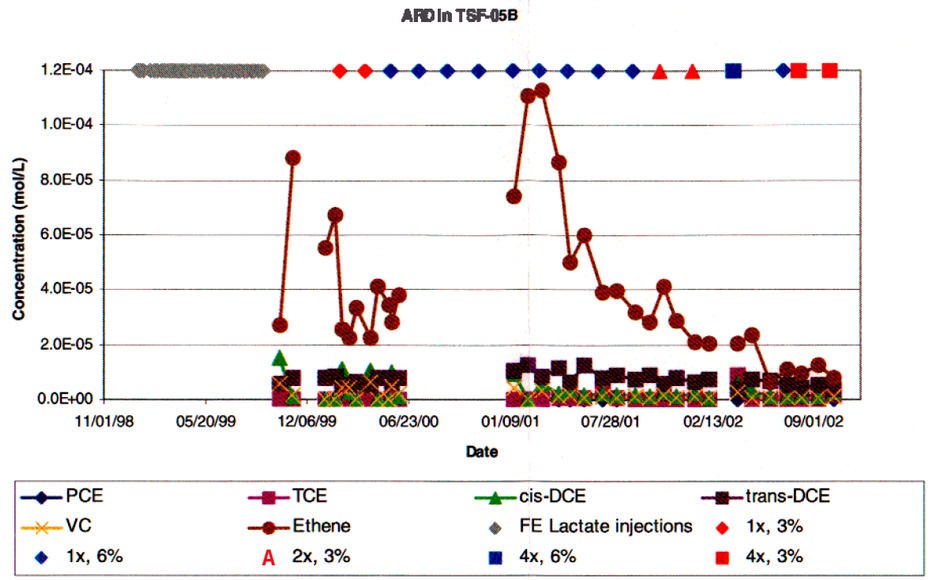

Figure 4-26. Anaerobic reductive dechlorination in TSF-05B.

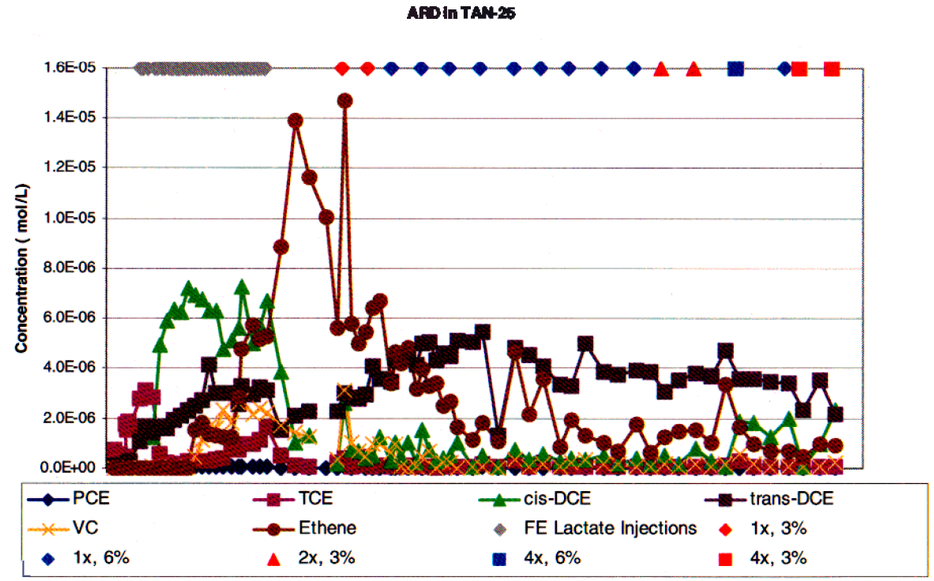

Figure 4-27. Anaerobic reductive dechlorination in TAN-25.

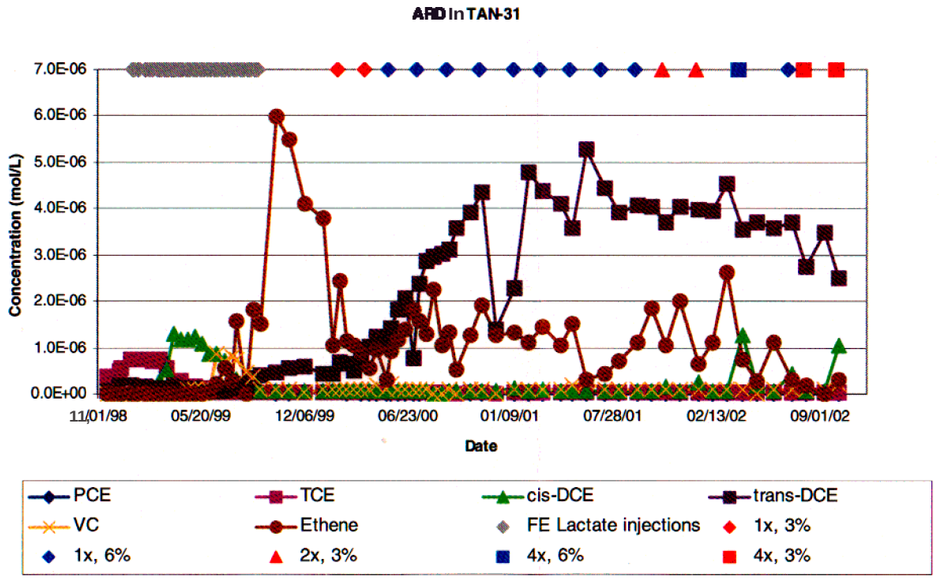

Figure 4-28. Anaerobic reductive dechlorination in TAN-31.

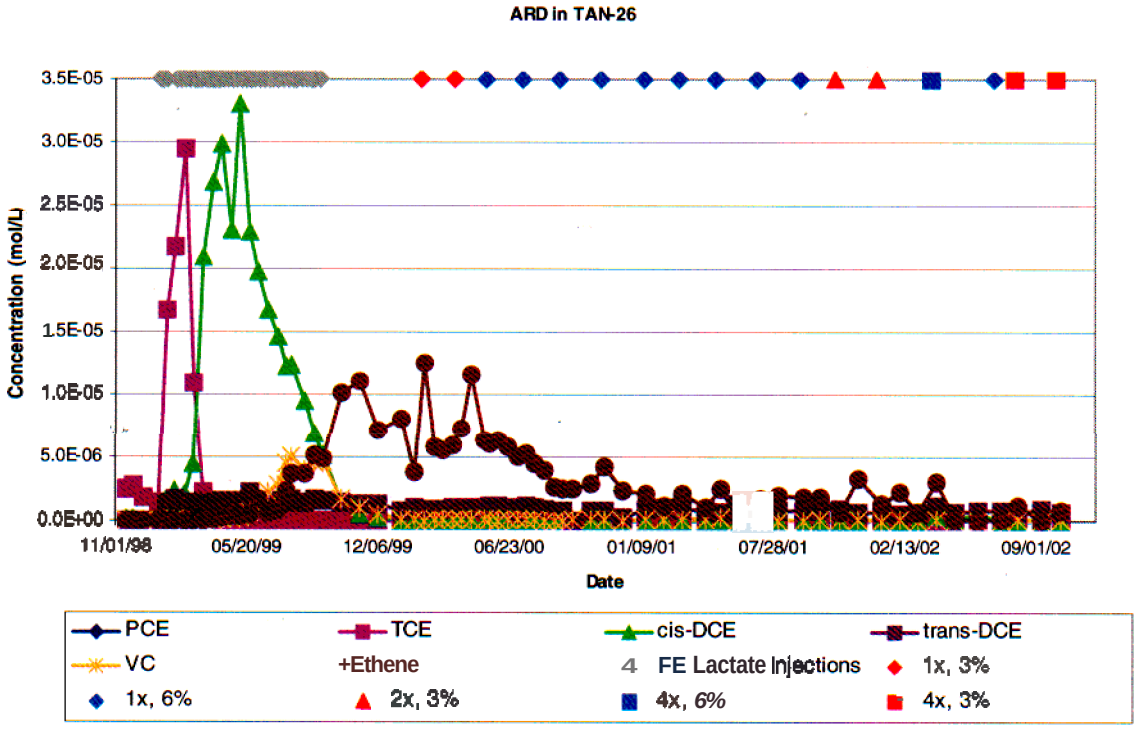

Figure 4-29. Anaerobic reductive dechlorination in TAN-26.

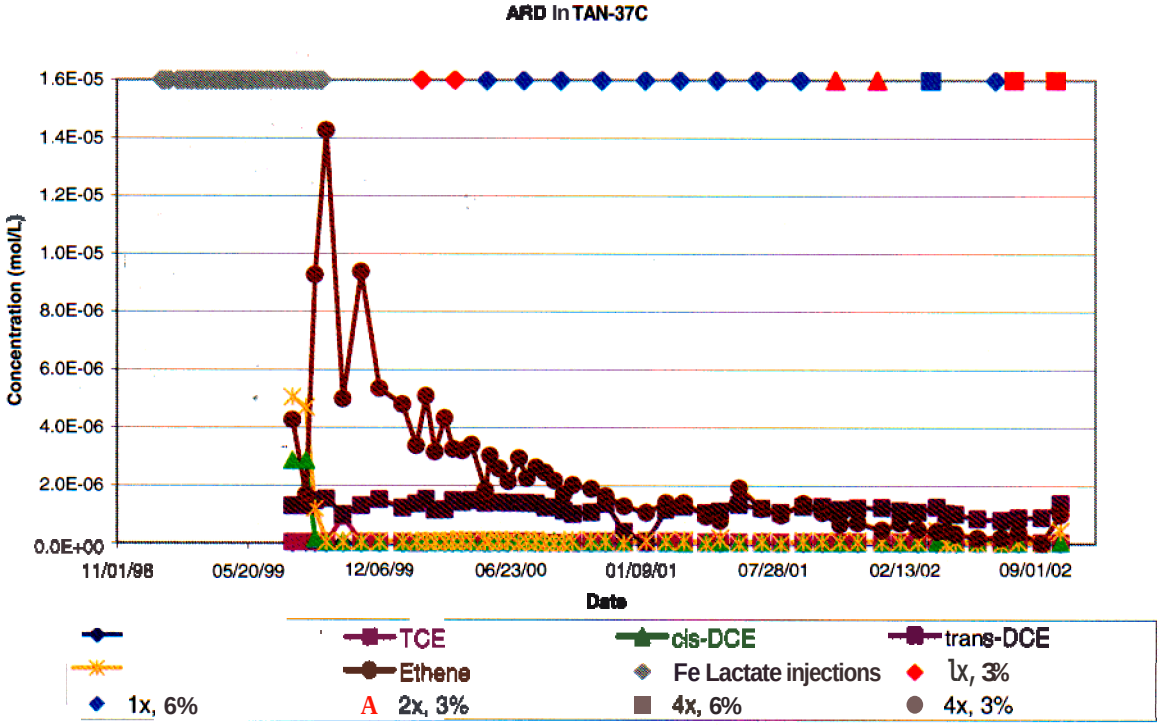

Figure 4-30. Anaerobic reductive dechlorination in TAN-37C.

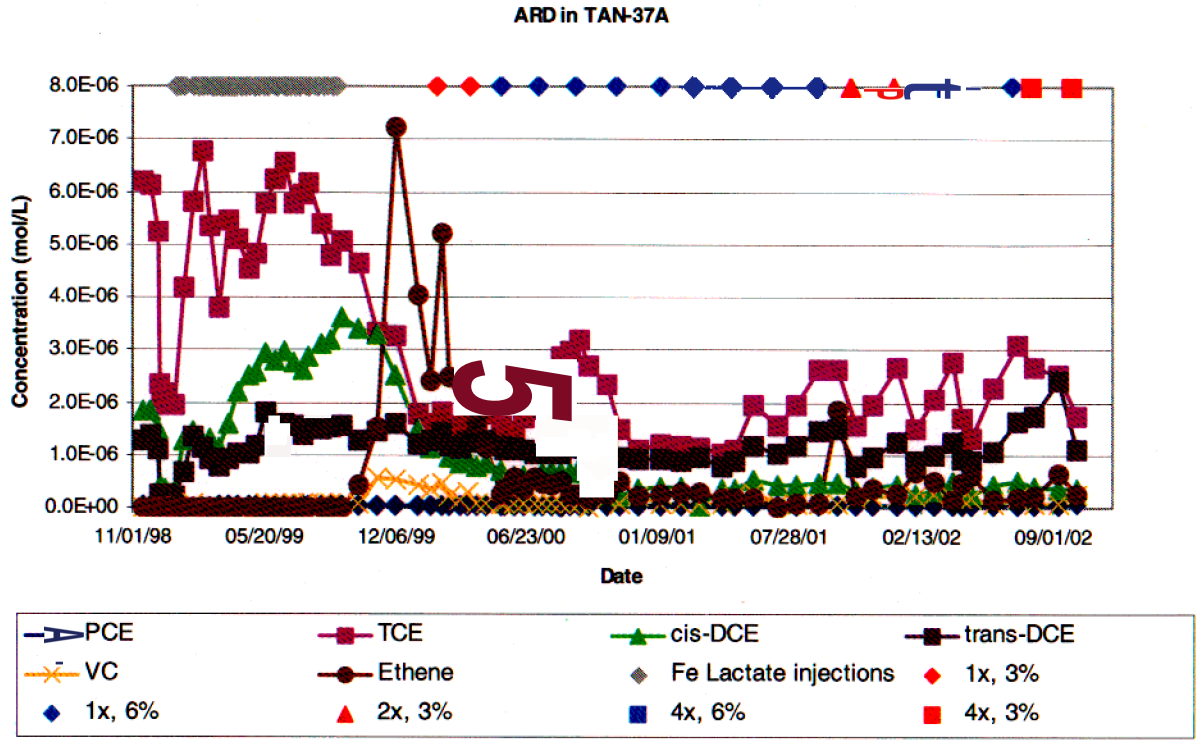

Figure 4-31. Anaerobic reductive dechlorination in TAN-37A.

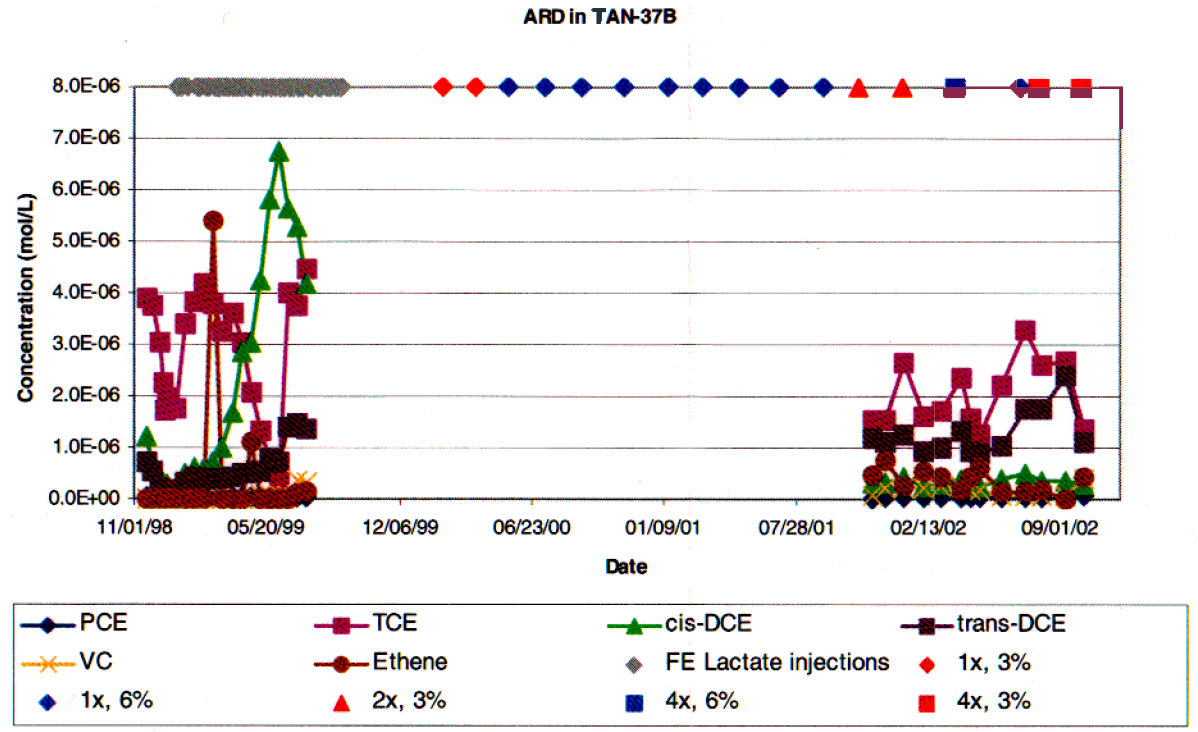

Figure 4-32. Anaerobic reductive dechlorination in TAN-37B.

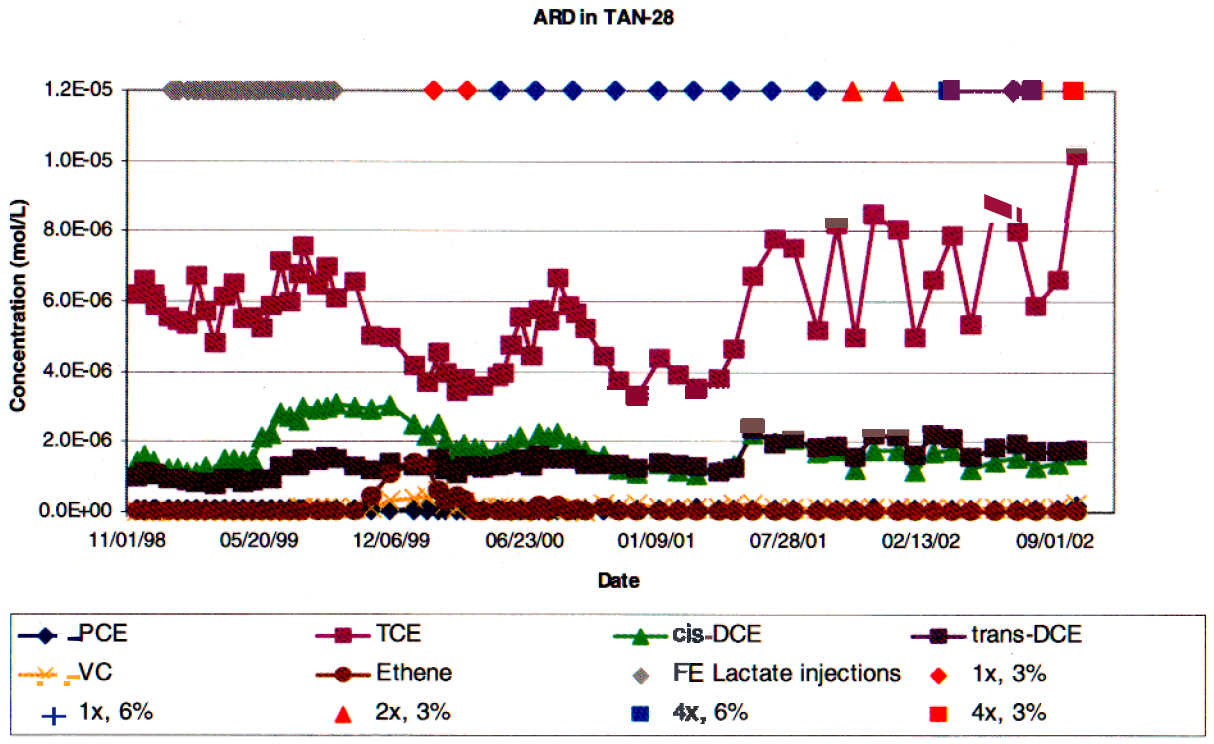

Figure 4-33. Anaerobic reductive dechlorination in TAN-28.

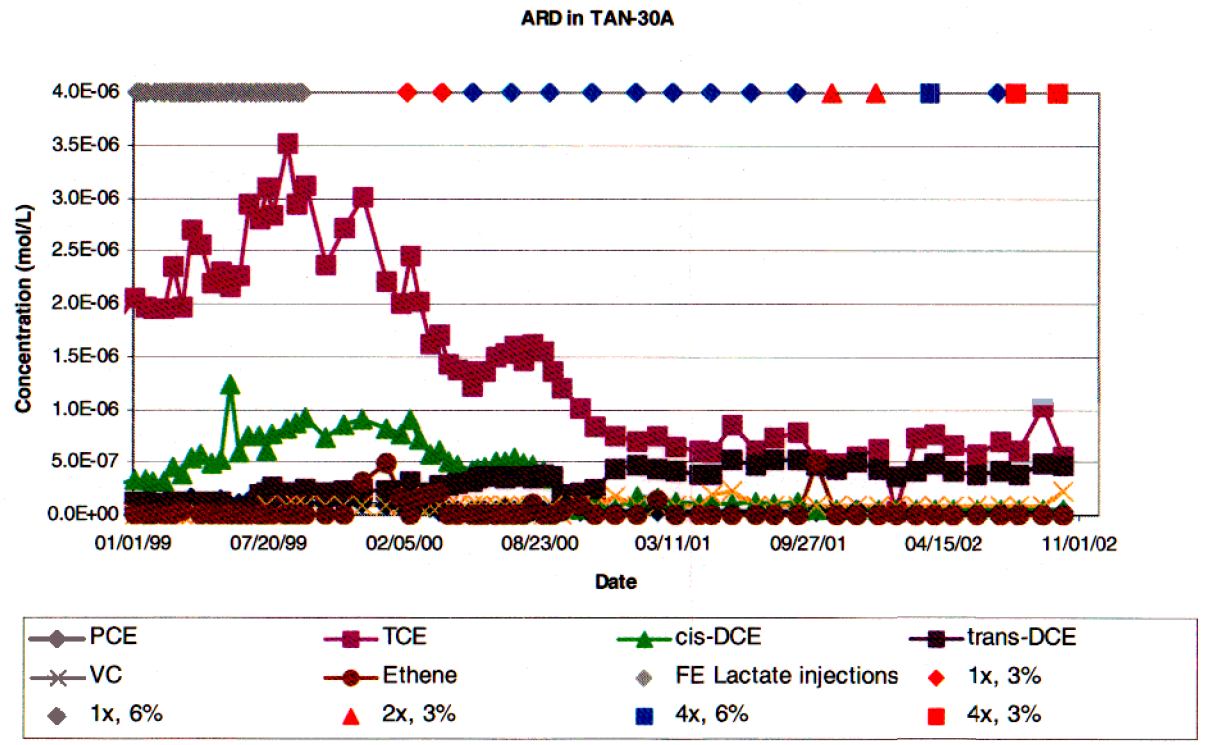

Figure 4-34. Anaerobic reductive dechlorination in TAN-30A.

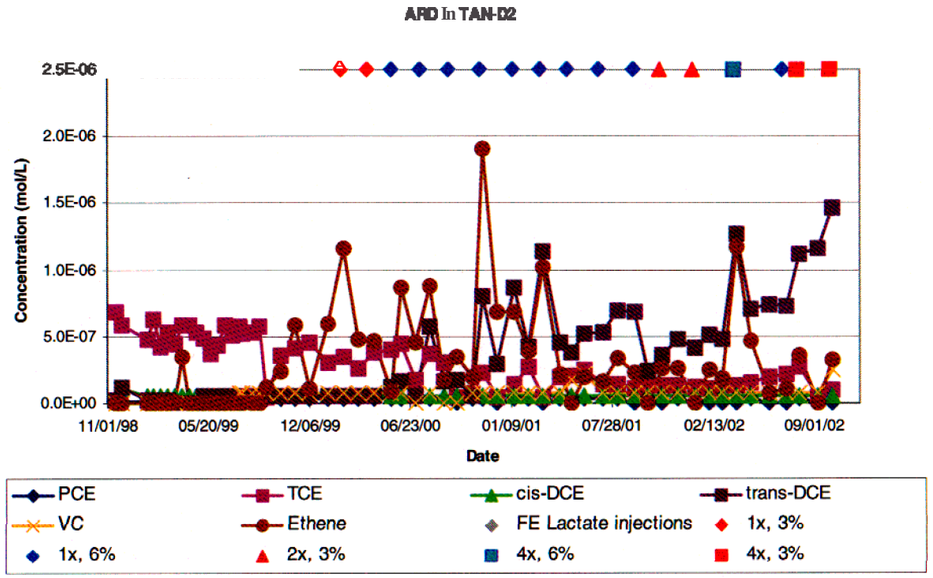

Figure 4-35. Anaerobic reductive dechlorination in TAN-D2.

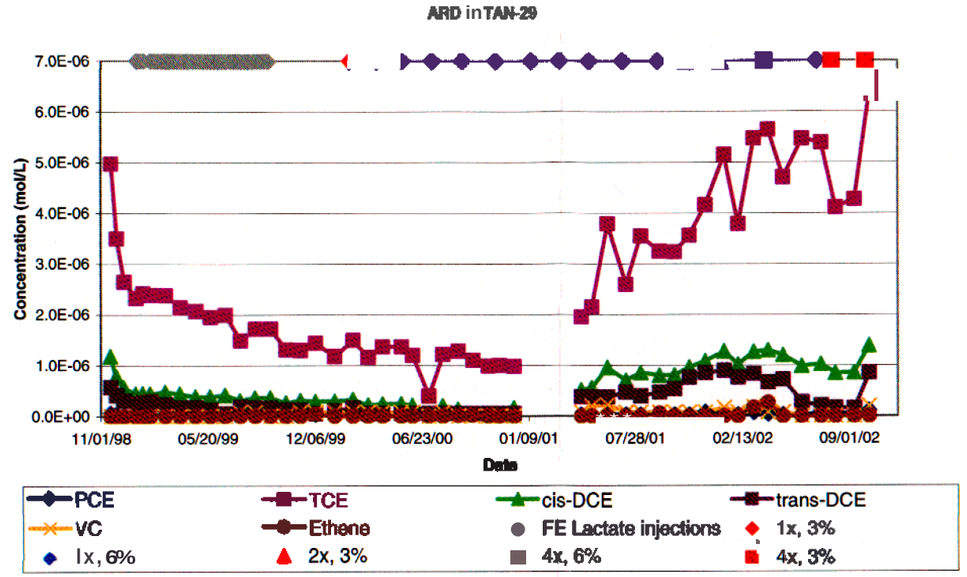

Figure 4-36. Anaerobic reductive dechlorination in TAN-29.

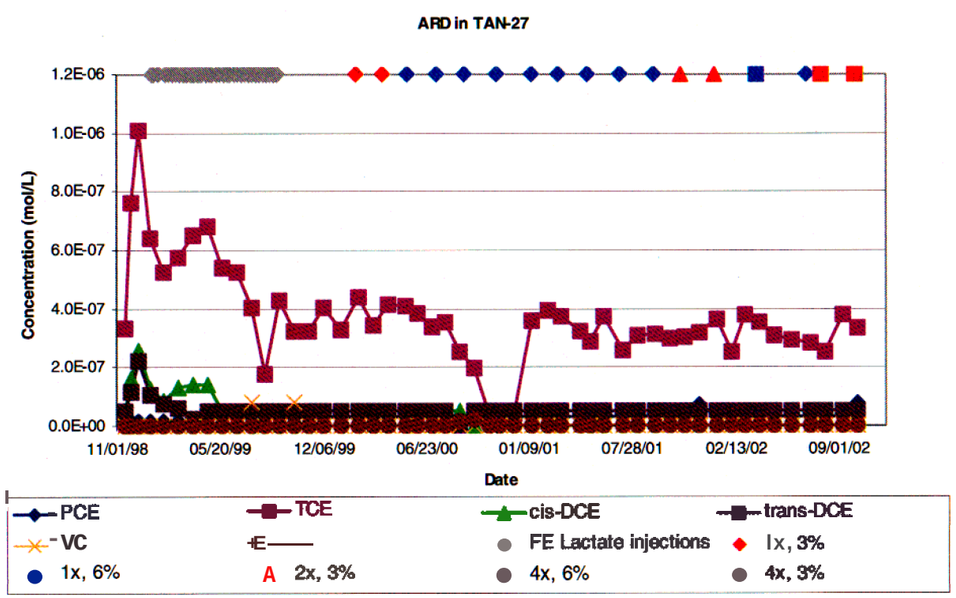

Figure 4-37. *Anaerobic* reductive dechlorination in TAN-27.

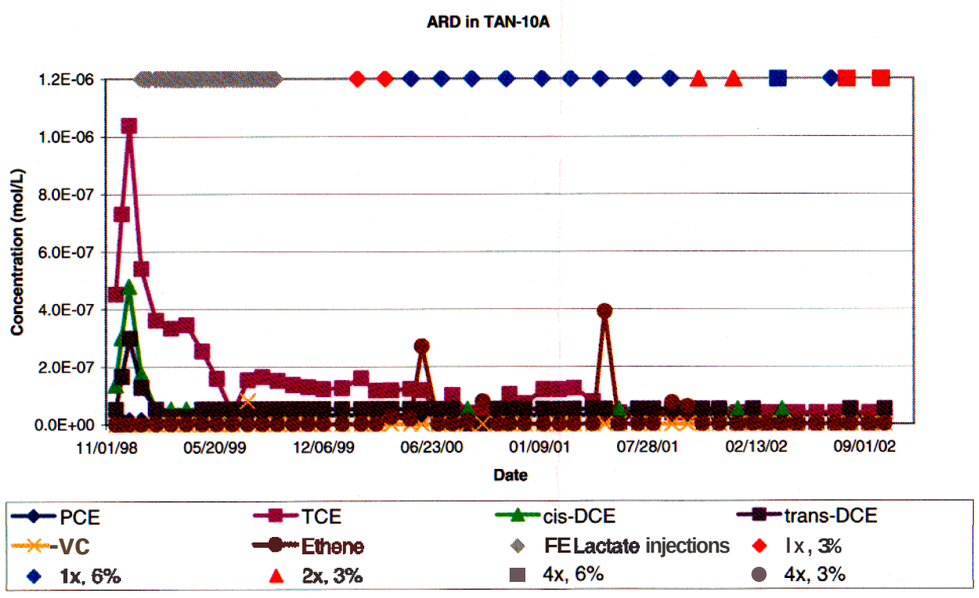

Figure 4-38. Anaerobic reductive dechlorination in TAN-10A.

Downgradient Wells—Volatile organic compound concentrations in downgradient wells have not changed significantly during the reporting period. Overall, no ARD was observed at these locations. TCE in TAN-28 continued to show a slight increasing trend, with the highest observed concentration (1,335 μg/L) since the start of the ISB field evaluation measured on October 7,2002. Degradation product concentrations have not changed at this location, with cis-DCE remaining around 175 μg/L and VC and ethene at nondetect levels. Trans-DCE remained relatively steady between 150 and 175 μg/L. VOC concentrations in TAN-30A are lower than TAN-28, but have remained relatively steady during the reporting period. TCE at this location ranged from 75 to 100 μg/L, while degradation products cis-DCE, VC, and ethene remained below detection limits. Trans-DCE concentrations remained steady at around 50 μg/L, below the MCL of 100 μg/L.

Volatile organic compound concentrations at TAN-37A and TAN-37B have remained relatively steady throughout the reporting period. TCE concentrations have been approximately 400 μg/L in both TAN-37A and TAN-37B. Concentrations of cis-DCE have also remained steady at approximately 30 μg/L. VC and ethene were near the lower detection limit in both locations. Trans-DCE was present at both locations at a concentration of around 100 μg/L, the MCL for this compound.

Outside Wells—Volatile organic compound concentrations in outside wells have shown little change during the reporting period. All VOCs in TAN-10A were below MCLs. VOCs in TAN-27 remained steady, with TCE levels around 40 μg/L. Sporadic detections of PCE have been observed at this location; however, these appeared to be isolated spikes rather than representative of an overall increasing trend. VOC concentrations in TAN-29 continued the increasing trend observed following the Air Stripper Treatment Unit (ASTU) shutdown in December 2000. TCE concentrations increased from about 400 μg/L in September 2001 to around 800 μg/L in October 2002, while cis-DCE and trans-DCE concentrations have fluctuated around 100 μg/L. VOC concentrations in TAN-D2 have fluctuated throughout the reporting period. TCE ranged from a high of approximately 36 μg/L to a low of less than the detection limit. Trans-DCE increased during the reporting period, ranging from a low of 24 μg/L to a high of 141 μg/L, with higher concentrations correlating to high volume injections.

Trans-DCE—Throughout ISB operations, trans-DCE has appeared recalcitrant to degradation relative to the other chloroethenes. Trans-DCE was highest at wells TSF-05A and TSF-05B, with concentrations around 500 μg/L. In general, concentrations decrease downgradient of TSF-05. Concentrations were approximately 300 to 400 μg/L in TAN-25 and 100 μg/L in TAN-37A. Concentrations appeared to increase slightly towards TAN-28, to 150 to 200 μg/L. Generally, the trans-DCE concentrations in the source area appeared to be decreasing, while trans-DCE in the downgradient and outside locations remained steady. The only location showing an increase, as of October 2002, was TAN-D2.

4.1.4 In Situ Monitoring

During this reporting period, multiparameter water quality instruments were deployed in source area wells TAN-25 and TAN-31, and in downgradient wells TAN-37 (A and B depths), TAN-28, and TAN-30A. Results of data collection and operational issues are presented below.

In the source area wells, spikes in specific conductance showed the distribution of the sodium lactate electron donor solution following each injection in TSF-05. The results from TAN-31 are shown as an example of the response in source area wells following injection (Figure 4-39). Following each increase, specific conductance values gradually decreased until the next sodium lactate injection. Temperature, pH, and ORP data were used to assess the aquifer conditions for ARD in the source area. As shown in Figure 4-39, at TAN-31 the temperature remained mostly between 14 and 14.5°C, and pH was, for the most part, between 6.5 and 7.5. (It should be noted that the temperature in TAN-31 is approximately 1.5 to 2.0 degrees higher than most other ISB wells.) The ORP probe requires a significant stabilization period after it is redeployed in a well. At TAN-31, ORP remained between -200 and -300 mV following this period of stabilization. Spikes in any of these parameters outside of the ranges may be the result of malfunctioning probes, problems with field standardizations, or from purging and sampling the well.

In the downgradient wells, increases in the specific conductance were not observed following each sodium lactate injection. The results from TAN-37A are presented as an example of the response in downgradient wells (Figure 4-40). As shown in Figure 4-40, the specific conductance remained rather stable between 0.9 to 1.1 mS/cm for TAN-37A. Similarly, the specific conductance values were between 0.84 and 0.95 mS/cm for both TAN-28 and TAN-30A, and 1.1 and 1.9 mS/cm for TAN-37B. Aquifer conditions in the downgradient wells show lower temperatures than TAN-31, ranging from 12.7 to 13.2°C, and higher pH ranges than the source wells, from between 6.9 to 9.5. ORP values were higher and exhibited greater fluctuation than seen in source area wells, from -344 to 475 mV.

During this reporting period, 7 Hydrolab MiniSonde units, 1 Hydrolab DataSonde unit, and 1 Hydrolab Diver were used for collection of in situ data. Operational issues with the MiniSonde units included sending six of the seven back to the manufacturer for maintenance and repair; three were sent back once, and three were sent back twice. Due to recurrent problems with Hydrolab equipment, In-Situ, Inc. TROLL 9000 multiparameter water quality instruments were purchased to replace the Hydrolabs for both in situ and purge data collection. Data collection using a Troll deployed in TAN-28 began on August 22, 2002. The remainder of the Troll telemetry system was installed on October 28, 2002.

4.1.5 Water Level Monitoring

Analysis of water level data in the 2001 ISB Annual Performance Report (INEEL 2002a) found discernable localized water level rises (i.e., mounding) in TSF-05, TAN-25, and TAN-31 resulting from sodium lactate injections in TSF-05. Therefore, water level measurements were collected during this reporting period for these three wells following the January 2, 2002; March 25, 2002; July 1, 2002; July 30, 2002; and October 1, 2002, sodium lactate injections. No water level data were collected following the September 5, 2002, and October 30, 2002, sodium lactate injections.

Figure 4-41 shows peak observed water level mounding for the three wells from March 1999 through October 2002. Prior to January 2002, the datalogger time step was 2 hours, which was not always sufficient to record the peak mounding following an injection. Following the January 2002 sodium lactate injection, the datalogger time step was 5 minutes; 10 minutes following the March through July injections; and 15 minutes following the October 2002 sodium lactate injection. Changes in injection volumes and rates that may affect the mounding response are also shown in Figure 4-41.

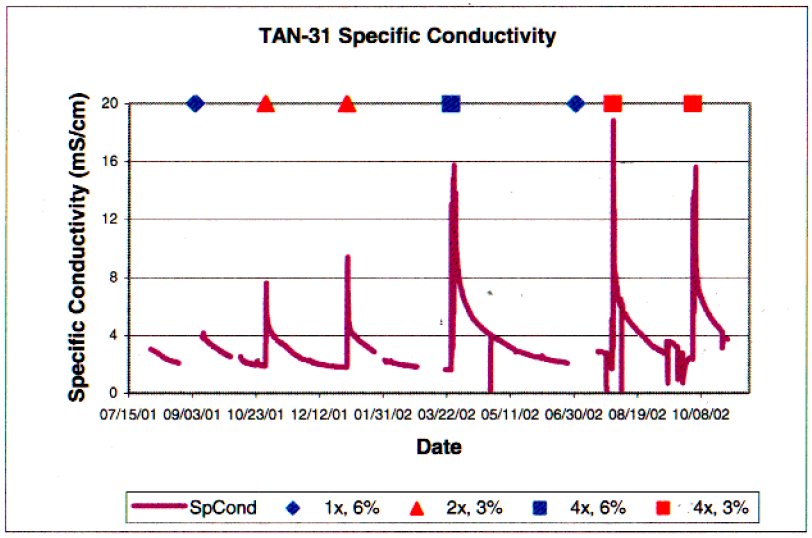

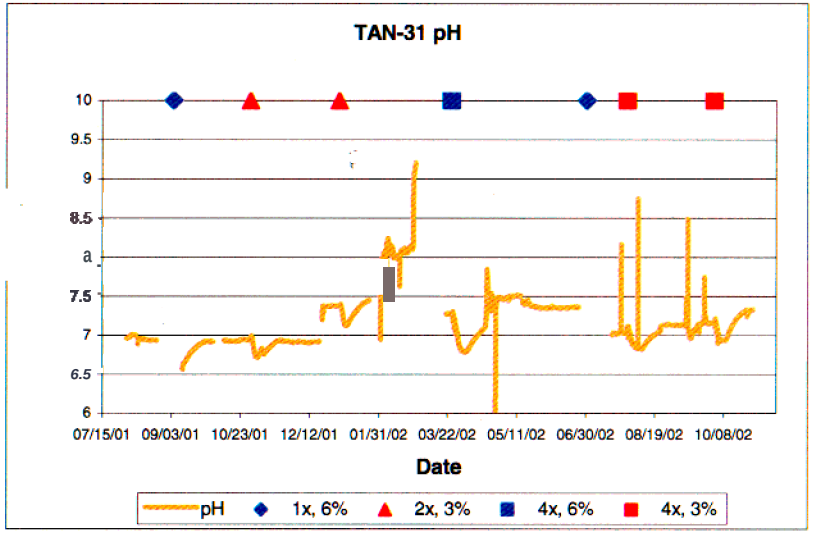

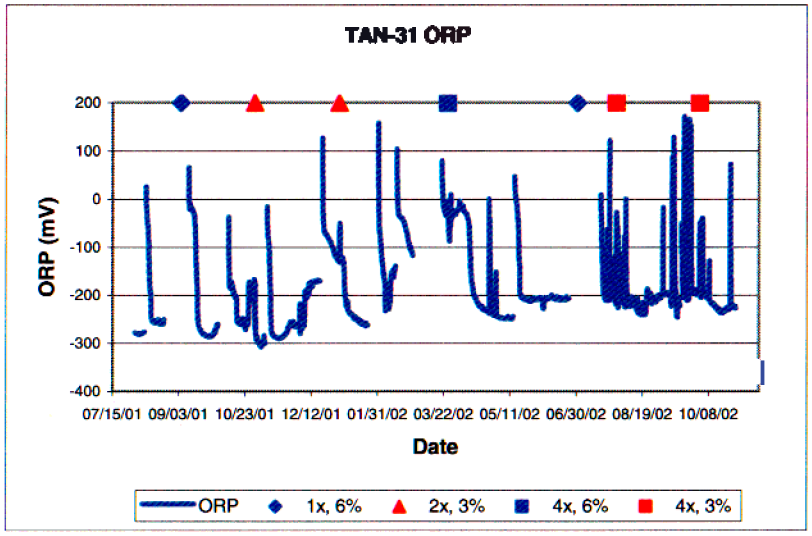

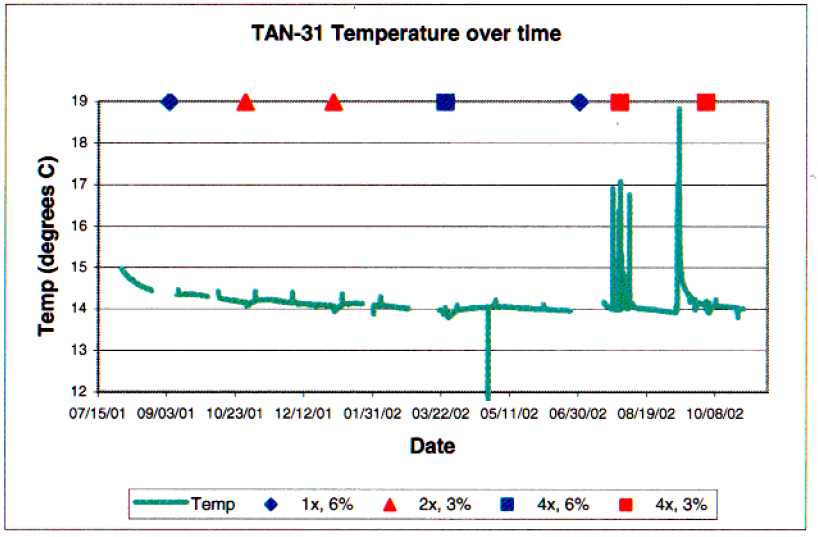

Figure 4-39. In situ monitoring results from TAN-31.

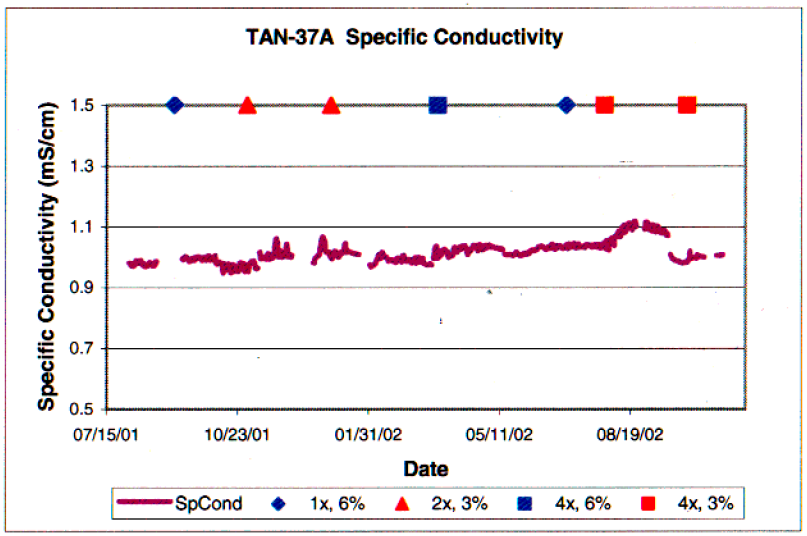

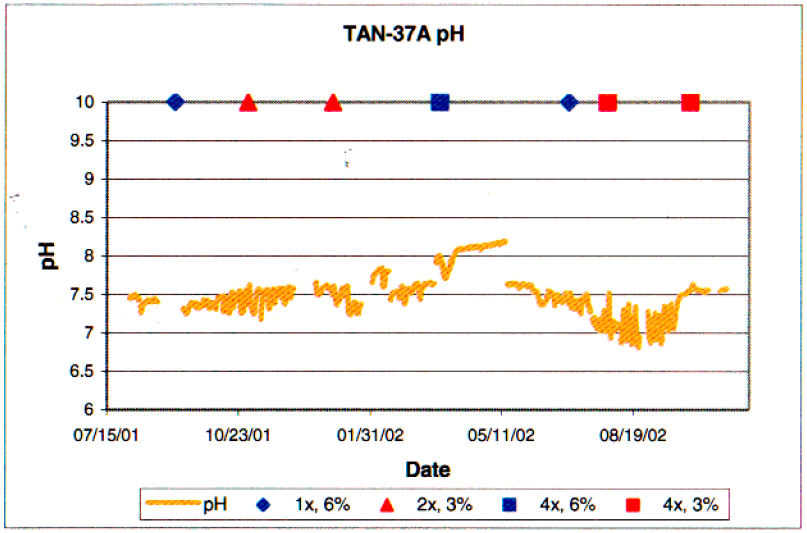

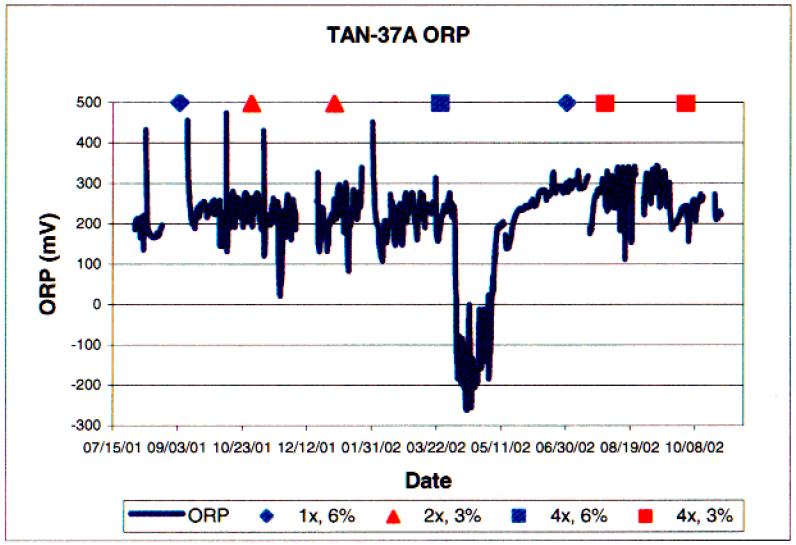

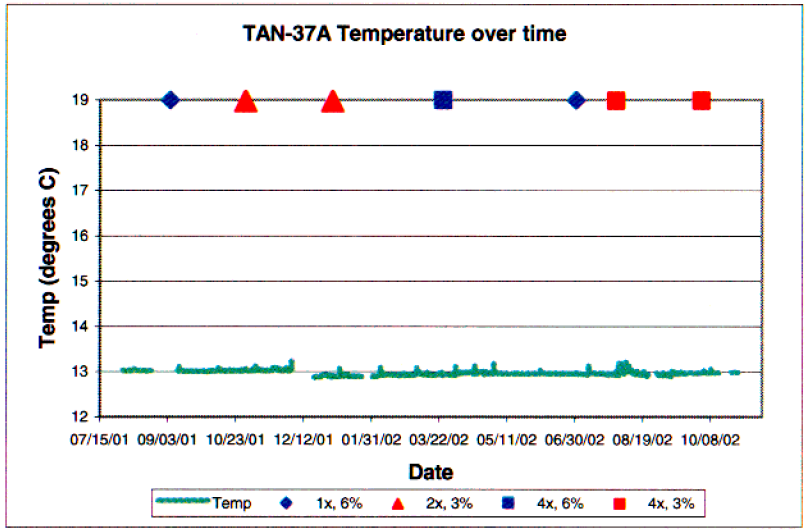

Figure 4-40. In situ monitoring results from TAN-37A.

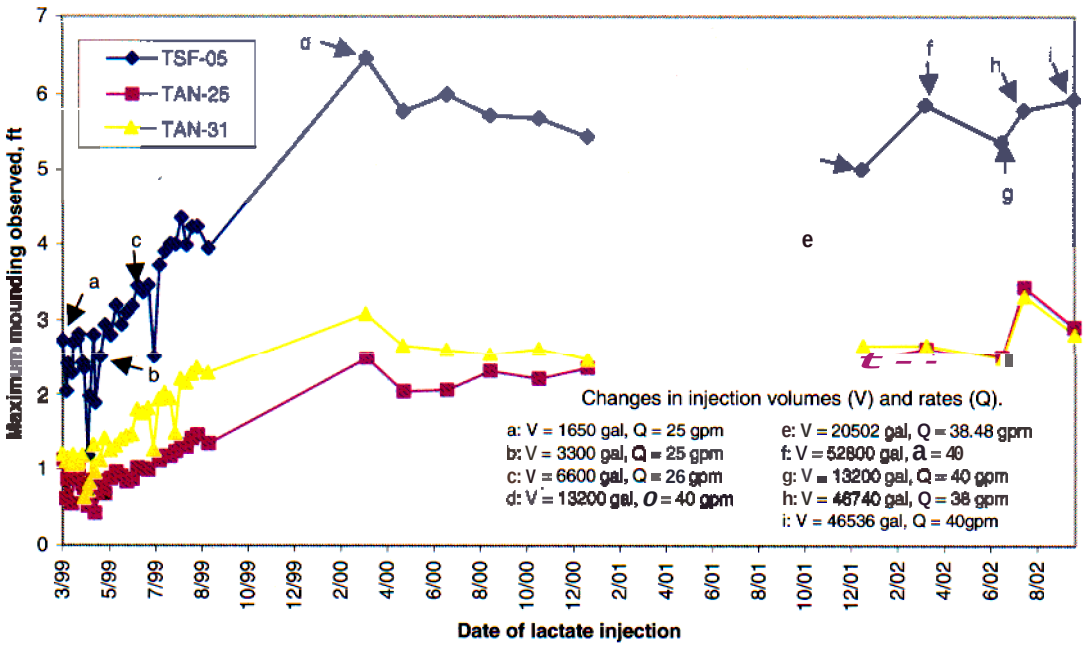

Figure 4-41. Peak water level mounding following sodium lactate injections.

As shown in Figure 4-41, mounding at TSF-05 has increased from approximately 2.5 ft in early 1999 to greater than 4.9 ft since March 2000. Mounding at TAN-25 and TAN-31 has also increased over time from approximately 1 ft in early 1999 to around 3 ft in October 2002. These increases in the peak mounding are almost certainly affected by the increased injection volumes used over time subsequent to the field evaluation.

Also of note is the observation that the difference in the peak mounding seen in TAN-25 and TAN-31 has changed over time. During the field evaluation, the peak mounding observed in TAN-31 was *0.5* to 0.75 ft greater than that observed in TAN-25. This difference began to decrease during PDP-II, and the peak mounding values observed at TAN-25 and TAN-31 beginning in January 2001 have been very similar. It appears that the peak mounding in TAN-31 has decreased slightly during PDP-II and PDO. This may be due to an increase in the effective porosity along the flow path from TSF-05 to TAN-31.

4.1.6 Metals and Radionuclides

One PDO objective was to determine whether sodium lactate injection resulted in mobilization of metals, strontium, and/or SVOCs from the secondary source during continued implementation of ISB system operations. Metals, radionuclides, and SVOCs are not amenable to recovery and/or treatment by air stripping in the NPTF; therefore, these contaminants could become groundwater compliance issues if mobilized. Mechanisms of mobilization could include:

- Increased hydraulic gradient produced by injection and downgradient extraction
- Increased solubility produced by pH decrease
- Changes in redox chemistry
- Changes in phase equilibria (induced desorption or dissolution) resulting from sodium lactate injection

- Ion exchange resulting from injecting high concentrations of sodium in sodium lactate.

During the last reporting period, data analysis results showed that mobilization of Sr-90 has occurred in a localized area around TSF-05; however, effects were not measurable or significant in downgradient wells. In addition, significant mobilization of metals and SVOCs had not occurred and no mobilization of Sr-90, metals, and SVOCs outside of the ISB treatment cell had been observed. SVOC monitoring was completed during the last reporting period with results reported in the 2001 ISB Annual Performance Report (INEEL 2002a).

To meet this PDO objective during this reporting period, concentrations of gamma emitters, alpha emitters, metals, and strontium were monitored at seven wells. Source area monitoring included TSF-05A, TSF-05B, TAN-25, and TAN-31. Conditions deep in the aquifer were monitored at TAN-26, downgradient monitoring at TAN-28, and outside monitoring at TAN-29. Tritium was monitored at all ISB wells. Results of monitoring and assessment of potential mobilization are discussed below. Data are included in Appendix D (see attached CD-ROM).

4.1.6.1 Gamma and Alpha Emitters. Gamma emitters were monitored on a quarterly basis during this reporting period and the results are presented in Appendix D (see attached CD-ROM). Cesium-137 was consistently detected in the source area wells. During this reporting period, Cesium-137 at TSF-05B was reported at levels between 615 to 1,730 pCi/L, TSF-05A between 420 to 1,130 pCi/L, TAN-25 between 472 and 798 pCi/L, and TAN-31 between 355 and 517 pCi/L. The MCL for Cesium-137 is 119 pCi/L. Other gamma emitters were sporadically detected or included a detectable error value in the source area and deep wells. No gamma emitters were detected in the downgradient or outside wells.

Alpha emitters were monitored once during this reporting period. The highest value, 16.3 pCi/L, was measured at TSF-05B. However, this was below the minimum detectable activity (MDA) of 50; therefore, this value was flagged as below detection. Minimum detectable activity values are different for each reported result. Values reported above the MDA were measured at TAN-28 and TAN-29, which reported values of 7.04 and 7.62 pCi/L, respectively. The MCL for alpha particles is 15 pCi/L, so these detections remain below the MCL value. Data are included in Appendix D (see attached CD-ROM).

4.1.6.2 Metals. Metals were monitored on a quarterly basis during this reporting. A summary of the results is presented here and a complete presentation of all the detections is included in Appendix D (see attached CD-ROM). Metals detected at the source area wells included barium, calcium, chromium, iron, magnesium, manganese, potassium, sodium, and zinc. Nickel was also detected at TSF-05A, TSF-05B, and TAN-25 and vanadium was detected at TSF-05B, TAN-25, and TAN-31. Of these, only two have established MCLs: barium and chromium. Barium was not detected above the MCL of 2 mg/L in any source area wells. Chromium was detected above the MCL of 0.1 mg/L at 107 and 204 mg/L at TAN-25 and TSF-05B, respectively, in a single sampling event (August 2002). Detected metals at TAN-26 included barium, calcium, iron, magnesium, manganese, nickel, potassium, sodium, and zinc. Metals detected at TAN-28 included barium, calcium, copper, magnesium, manganese, potassium, sodium, and zinc. At TAN-29, detected metals included barium, calcium, cadmium, copper, iron, magnesium, manganese, nickel, potassium, sodium, and zinc. None of these metals were detected above MCLs.

4.1.6.3 Strontium. As reported in the 2001 ISB Annual Performance Report (INEEL 2002a), data analysis showed mobilization of Sr-90 in a localized area around TSF-05. For the current report, Sr-90 data from the nearly 4 years of ISB operations were compared to pre-ISB Sr-90 data for ISB wells. Figure 4-42 shows Sr-90 plotted from 1996 to August 2002 for selected ISB wells (pre-ISB TSF-05 data was plotted as TSF-05A). Figure 4-42 shows that ISB operations have increased Sr-90 concentrations in TSF-05, TAN-25, and TAN-26 by nearly an order of magnitude compared to pre-ISB levels. In addition, Sr-90 concentrations in TAN-37 have increased by a factor of two.

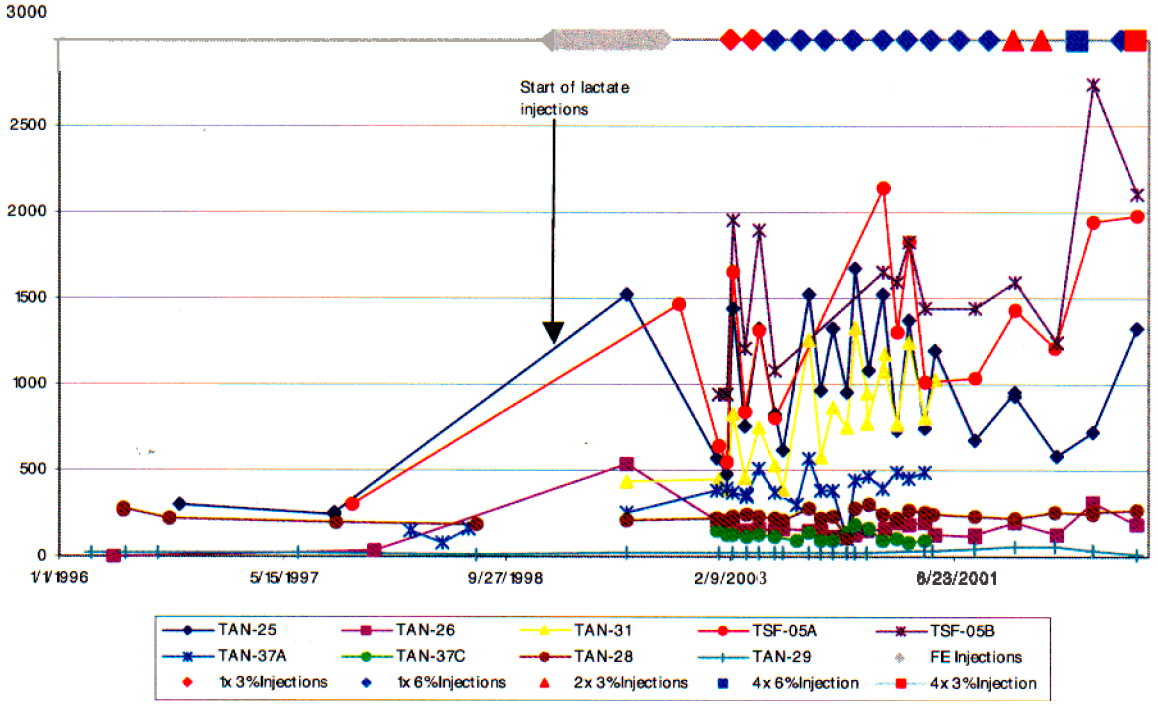

Figure 4-42. Strontium results for select wells.

However, the Sr-90 concentrations in all other ISB wells have remained near pre-ISB levels. This indicates *that* although increased Sr-90 mobilization has occurred over a very localized area near TSF-05 due to ISB operations, the increased concentrations have historically been and continue to be rapidly attenuated such that no Sr-90 increases have been observed downgradient of TAW-37. A complete presentation of all strontium data is included in Appendix D (see attached CD-ROM).

4.1.6.4 Tritium. Tritium data were collected on a monthly basis during this reporting period for all ISB wells. Tritium concentrations throughout the ISB treatment cell were all below MCL values. *All* tritium data collected during the reporting period are presented in Appendix D (see attached CD-ROM).

4.1.7 Quality Assurance

Quality assurance/quality control (QA/QC) measures are implemented as part of the data collection process to monitor precision, accuracy, and completeness for all ISB data. Precision was evaluated through performance of duplicate samples at the IRC laboratory, ISB field laboratory, and all off-Site laboratories. Accuracy was gauged through performance of standards, standard additions, matrix spikes and matrix spike duplicates (MS/MSDs), performance evaluation (PE) samples, and blanks. All QA/QC results are presented in Appendix F.

The relative percent difference (RPD) was calculated for all duplicate samples to evaluate precision. The average RPD values for all ISB field analyses were within quality acceptance criteria. All IRC laboratory analyses were within the quality acceptance criteria, with the exception of ethene, which was slightly above the limit. *All* of the off-Site analyses were within the quality acceptance criteria, with the exception of PCE, VC, and methane. Radionuclides and metals analyses met the precision acceptance criteria.

Accuracy was evaluated through performance of standards, standard additions, MS/MSDs, splits, PE samples, and blanks. Standards and standard additions were performed in the ISB field laboratory.

Quality acceptance criteria for standards and standard additions were met for all analytes for which acceptance limits were defined. Matrix spike and matrix spike duplicate analyses for VOCs were performed at the IRC laboratory and the off-Site laboratories. No criteria were specified in the PDO SAP for MS/MSD data; future criteria have been established in the ISB Groundwater Monitoring Plan (INEEL 2003a). All MS/MSD data met these future criteria.

Splits were performed for VOCs and ethene/ethane/methane. Of these parameters, only trans-DCE was within the acceptance limits defined in the PDO SAP. Although many of the high RPDs for split samples could be attributed to the low magnitude of reported concentrations, the unacceptable splits results were the primary motivation for implementing the PE sampling program during this reporting period. High range and low range VOC PE samples were sent monthly to the IRC laboratory and quarterly to the off-Site laboratory (Severn Trent Laboratories), and results were generally within tolerance ranges, with the exception of one off-Site sample. Complete PE results are discussed in Appendix F. Trip blanks and field blanks were collected as an additional accuracy check. The only blank that was above detection was the July 2002 Tritium sample, which was 2,000 pCi/L. Completeness for the reporting period was 96.9%, exceeding the goal of 90%, as shown in Table 4-14.

4.2 Lactate Metals Results

Environmental Protection Agency TAL metals in sodium lactate were monitored in three batches of sodium lactate ordered from JRW Technologies; two batches during this reporting period, and one batch before August 2001. Analysis results were provided by JRW and are summarized in Table 4-15. Results are shown for filtered and nonfiltered samples and compared to allowable injected concentrations, defined for the field evaluation as 10 x MCL (DOE 1998, Attachment 1). Prior to analysis, the stock 60% (by weight) sodium lactate samples were diluted 1:10 v/v with deionized (DI) water, which resulted in a 6% nominal concentration.

As shown in Tables 4-15 through 4-17, the JRW product met all acceptance criteria (<10 x MCL) for TAL metals. Therefore, as long as JRW is used as the only sodium lactate vendor, no additional sodium lactate metals analyses will be performed. If sodium lactate is ordered from a different vendor, then sodium lactate metals analyses will be conducted for the first three batches ordered from the new vendor to ensure metals meet acceptance criteria.

4.3 Groundwater Modeling Results

As described in Section 3.4, groundwater modeling was used to create a predictive tool that can be used to simulate the COD distribution under various injection strategies. This section summarizes the results of the modeling activities, including the result of the calibration activities (Section 4.3.1) and the simulation of two injection scenarios (Section 4.3.2). A complete presentation of the results can be found in the TAN Groundwater Development and Initial Performance Simulation Report (INEEL 2002d).

4.3.1 Model Calibration Results

As described in Section 3.4, several calibration steps were used to develop the model. These included calibration of the transport model to observed water level changes during injection, calibration of the particle tracking component using specific conductance data following injections, and calibration of the observed COD distribution following an injection. The following information summarizes the results of these calibration activities. A complete description of the results is presented in the TAN Groundwater Development and Initial Performance Simulation Report (INEEL 2002d).

Table 4-14. Completeness for the reporting period.

Date	Number of Planned Samples[a]	Number of Planned Samples Collected	Percent (%) Complete for Planned Samples	Total Samples Collected[b]	Comments
6–8 Aug 01	166	166	100	177	12 microbiological samples added, 11 of those 12 were collected.
10–11 Sept 01	110	110	100	121	13 microbiological samples added; 11 of those 13 were collected. Field blank sample added for VOAs.
8 and 10 Oct 01	121	119	98.3	—	Samples not collected included one trip blank for ethenelethanelmethaneand one trip blank for VOAs. These blanks were not needed because only two deliveries were made to the IRC rather than the projected three deliveries.
5–7 Nov 01	193	193	100	—	—
19 Nov 01	14	14	100	—	—
3–6 and 10 Dec 01	126	124	98.4	—	Two microbiological samples not collected from TAN-25.
7–9 Jan 02	126	124	98.4	125	Samples not collected included one trip blank for ethenelethanelmethaneand one trip blank for VOAs, which were mistakenly left out of the IRC delivery. One microbiological sample added for TAN-37B.
4–6 Feb 02	189	189	100	—	—
4–5 Mar 02	113	103	91.2	—	Samples were not collected from TSF-05B due to an inoperable pump. One trip blank for ethenelethanelmethaneand one trip blank for VOAs were mistakenly left out of the IRC delivery.
1–3 Apr 02	119	118	99.2	—	One microbiological sample not collected from TAN-25.
17 Apr 02	28	28	100	—	—
29 Apr–1 May 02	183	182	99.5	—	One microbiological sample not collected from TAN-25.
8 May 02	9	6	66.7	—	Three microbiological samples not collected from TAN-25.
3–4 Jun 02	122	118	96.7	—	Two microbiological samples not collected from TAN-25. One trip blank for ethenelethanelmethanewas mistakenly left out of the IRC delivery and one trip blank was not needed.
8–10 Jul 02	118	118	100	—	—
5–6 Aug 02	184	181	98.4	—	Samples not collected included one trip blank for ethenelethanelmethaneand one trip blank for VOAs. These blanks were not needed because only two deliveries were made to the IRC rather than the projected three deliveries. One PE sample was not used.
9 Sept 02	125	121	96.8	123	Samples not collected included two trip blanks for ethenelethanelmethaneand two trip blanks for VOAs. Two iodide samples were added.
7–8 Oct 02	118	118	100	120	Two iodide samples were added.
Average			96.9		

a. Represents the number of planned samples shown on the SAP table
b. Represents the total samples collected during that sampling event in the cases where more samples were collected than what was planned (see the comments section for details).
VOA = volatile organic analyte.

Table 4-15. Sodium lactate metals results for June 7. 2002

Target Analyte Metals	Safe Drinking Water Limits	Allowable Injected Concentration	Stated in TOS 1214R1	JRW Wilclear 1:10 v/v, Unfiltered ug/L 6/7/02			JRW Wilclear 1:10 v/v, Filtered ug/L 6/7/02		
TAL metal	SDWA MCLs, ug/L	10 x MCLs	RDLs, ug/L	28151B-1	28151B-2	28151B-3	28151B-4	28151B-5	28151B-6
Al	NA	NA	200	3210	3670	3480	1690 B	3190	2860
Sb	6a, b	60	6	10.0 u	10.0 u	10.0 u	10.0 u	10.0 u	10.0 u
As	50c	500	50	50.0 U	50.0 U	50.0 U	50.0 U	50.0 U	50.0 U
Ba	2000a, b	20000	100	53.7 B	61.2 B	61.8 B	50.0 U	69.0 B	50.5 B
Be	4a, b	40	4	8.0 u	8.0 u	8.0 u	8.0 u	8.0 u	8.0 u
Cd	5a, b	50	5	5.0 U	5.0 U	5.0 U	5.0 U	5.0 U	5.0 U
Ca	NA	NA	200	437 B	883 B	439 B	861 B	725 B	606 B
Cr	100a, b	1000	100	208 B	225 B	233 B	148 B	231 B	172 B
c o	NA	NA	110	50.0 U	50.0 U	50.0 U	50.0 U	50.0 U	50.0 U
Cu	1300b, d	13000	80	50.0 U	62.8 B	54.8 B	63.9 B	82.6 B	50.0 U
Fe	NA	NA	1000	944 B	977 B	1040 B	701 B	1060 B	692 B
Pb	15d, Ob	150	15	5.0 U	5.0 U	5.0 U	5.0 U	5.0 U	5.0 U
Mg	NA	NA	200	200 u	200 u	200 u	200 u	200 u	200 u
Mn	NA	NA	40	44.3 B	52.3 B	52.0 B	40.0 U	54.1 B	40.0 U
Hg	2a, b	20	2	10.0 u	10.0 u	10.0 u	10.0 u	10.0 u	10.0 u
Ni	NA	NA	100	128 B	124 B	127 B	88.3 B	126 B	94.3 B
K	NA	NA	1000	21400	49600	99500	19600	45100	40800
Se	50a, b	500	50	50.0 U	50.0 U	50.0 U	50.0 U	50.0 U	50.0 U
Ag	NA	NA	10	5.0 U	5.0 U	5.0 U	5.0 U	5.0 U	5.0 U
Na	NA	NA	1000	152000000	156000000	163000000	79500000	153000000	155000000
Tl	2a, 0.5b	20	2	3.0 U	3.0 U	3.0 U	3.0 U	3.0 U	3.0 U
V	NA	NA	100	50.0 U	50.0 U	50.0 U	50.0 U	50.0 U	50.0 U
Zn	NA	NA	100	50.0 U	50.0 U	50.0 U	164 B	74.4 B	50.0 U

a. 40 CFR 141.62
b. 40 CFR 141.55, MCLGs
c. 40 CFR 141.11
d. 40 CFR 141.80

Date qualifiers:
U = Analyte was analyzed for but not detected
B = Value is less than the CRDL but greater than the IDL.

Table 4-16. Sodium lactate metals results from October 1. 2001.

Target Analyte Metals	Safe Drinking Water Limits	Allowable Injected Concentration	Stated in TOS 1214R1	JRW Wilclear 1:10 v/v, Unfiltered ug/L 10101/01			JRW Wilclear 1:10 v/v, Filtered ug/L 10101/01		
TAL metal	SDWA MCLs, ug/L	10 x MCLs	RDLs, ug/L	27734A-1	27734A-2	27734A-3	27734A-4	27734A-5	27734A-6
Al	NA	NA	200	6750	6940	6980	6790	6990	6830
Sb	6a, b	60	6	5.0 U	5.0 U	5.0 U	5.0 U	5.0 U	5.0 U
As	50c	500	50	50.0 U	50.0 U	50.0 U	50.0 U	50.0 U	50.0 U
Ba	2000a, b	20000	100	50.0 U	50.6 B	50.0 U	55.1 B	68.8 B	52.5 B
Be	4a, b	40	4	4.0 U	4.0 U	4.0 U	4.0 U	4.0 U	4.0 U
Cd	5a, b	50	5	5.0 U	5.0 U	5.0 U	5.0 U	5.0 U	5.0 U
Ca	NA	NA	200	440 B	409 B	430 B	412 B	901 B	440 B
Cr	100a, b	1000	100	159 B	163 B	162 B	165 B	165 B	164 B
co	NA	NA	110	50.0 U	50.0 U	50.0 U	50.0 U	50.0 U	50.0 U
Cu	1300b, d	13000	80	50.0 U	50.0 U	50.0 U	50.0 U	50.0 U	50.0 U
Fe	NA	NA	1000	1620 B	1650 B	1610 B	1660 B	1730 B	1730 B
Pb	15d, Ob	150	15	5.0 U	5.0 U	5.0 U	5.0 U	5.0 U	5.0 U
Mg	NA	NA	200	501 B	485 B	496 B	497 B	511 B	561 B
Mn	NA	NA	40	104 B	106 B	106 B	107 B	111 B	105 B
Hg	2a, b	20	2	2.0 u	2.0 u	2.0 u	2.0 u	2.0 u	2.0 u
Ni	NA	NA	100	103 B	116 B	119 B	108 B	113 B	114 B
K	NA	NA	1000	7050 B	11600	11800	10400	9510 B	7660 B
Se	50a, b	500	50	50.0 U	50.0 U	50.0 U	50.0 U	50.0 U	50.0 U
Ag	NA	NA	10	6.0 U	6.0 U	6.0 U	6.0 U	6.0 U	6.0 U
Na	NA	NA	1000	152000000	148000000	159000000	144000000	141000000	143000000
Tl	2a, 0.5b	20	2	2.5 U	2.5 U	2.5 U	2.5 U	2.5 U	2.5 U
V	NA	NA	100	50.0 U	50.0 U	50.0 U	50.0 U	50.0 U	50.0 U
Zn	NA	NA	100	50.0 U	50.0 U	50.0 U	69.2 B	119 B	54.5 B

a. 40 CFR 141.62
b. 40 CFR 141.55, MCLGs
c. 40 CFR 141.11
d. 40 CFR 141.80

Date qualifiers:
U = Analyte was analyzed for but not detected.
B = Value is less than the CRDL but greater than the IDL.

Table 4-17. Sodium lactate metals results for March 16. 2001

Target Analyte Metals	Safe Drinking Water Limits	Allowable Injected Concentration	Stated in TOS 1214 R1	JRW Unfiltered Sample Results ug/L 3/16/01			JRW Filtered Sample Results ug/L 3/16/01		
TAL metal	SDWA MCLs, ug/L	10 x MCLs	RDLs, ug/L	27404C-1	27404C-2	27404C-4	27404C-3	27404C-5	27404C-6
Al	NA	NA	200	2110	2180	2230	2140	1690B	1950 B
Sb	6a, b	60	6	6 U	6 U	6 U	6 U	6 U	6 U
As	50c	500	50	50 U	50 U	50 U	50U	50 U	50 U
Ba	2000a, b	20000	100	50 U	50 U	57.6 B	50U	57.1 B	51.1 B
Be	4a, b	40	4	3 u	3 u	3 u	3 u	3 u	3 u
Cd	5a, b	50	5	3 u	3 u	3 u	3 u	3 u	3 u
Ca	NA	NA	200	327 B	279 B	317 B	263 B	687 B	322 B
Cr	100a, b	1000	100	52 B	65.3 B	50 U	70.5 B	61.6 B	50 U
c o	NA	NA	110	50 U	50 U	50 U	50 U	50 U	50 U
Cu	1300b, d	13000	80	50 U	63.1 B	59.6 B	62.9 B	50 U	50 U
Fe	NA	NA	1000	850 B	1290 B	776 B	1140 B	1060 B	800 B
Pb	15d, Cb	150	15	3 u	5.6 B	3 u	3 u	3 u	3.6 B
Mg	NA	NA	200	282 B	266 B	260 B	200 u	407 B	306 B
Mn	NA	NA	40	40 U	40 U	40 U	40 U	40 U	40 U
Hg	2a, b	20	2	2 u	2 u	2 u	2 u	2 u	2 u
Ni	NA	NA	100	62.8 B	69.3 B	67.9 B	64.8 B	76.7 B	66.5 B
K	NA	NA	1000	1000 u	10900	11800	11500	16200	13800
Se	50a, b	500	50	30 U	30 U	30 U	30 U	30 U	30 U
Ag	NA	NA	10	5 u	5 u	5 u	5 u	5 u	5 u
Na	NA	NA	1000	154000000	148000000	150000000	153000000	149000000	148000000
Tl	2a, 0.5b	20	2	1.8 u	1.8 u	1.8 u	1.8 u	1.8 u	1.8 u
V	NA	NA	100	50 U	50 U	50 U	50 U	50 U	50 U
Zn	NA	NA	100	74.6 B	67.7 B	87.5 B	71.2 B	106 B	82.5 B

a. 40 CFR 141.62
b. 40 CFR 141.55, MCLGs
c. 40 CFR 141.11
d. 40 CFR 141.80

Date qualifiers:
U = Analyte was analyzed for but not detected.
B = Value is less than the CRDL but greater than the IDL.

The model simulated head change fit data for some wells reasonably well, but not at well TAN-31, where an unexpected response was reported in the field. Local scale heterogeneities may be the cause of the anomaly. The model-simulated COD concentration curves had the same general shape as the field data if the peak arrival times from the specific conductance measurements are included, but the model values were higher. Insufficient field data restricted the ability to determine the ranges of key transport parameters adequately; good observed COD breakthrough curves were not available. That deficiency somewhat limits the model's ability to reliably predict future conditions, but the model's mass balance feature is quite useful in considering the extent of potential electron donor distribution (INEEL 2002d).

4.3.2 Injection Scenario Simulation Results

As described in Section 3.4, Scenario 1 involved the injection of the same mass as the PDP-II injections (1,320 gal 60% sodium lactate) but at half the concentration (~3% sodium lactate). For Scenario 1, the results are similar to those obtained with the PDP-II injection rates. This suggests that the more dilute sodium lactate injections yield about the same results as the PDP-II injections in terms of COD distribution. Scenario I simulated results fall within a factor of 2 of the observed concentrations for TSF-05B. At the observation wells, the first post-injection observed concentrations, about 6 days after injection, fall on or very near the simulated concentration time series curves. The simulated results were still significantly higher than the observed concentrations 30 to 35 days following injection, suggesting that the model COD decay rates were too low.

Scenario 2 involved injection of dilute concentrations at a hypothetical well just west of TAN-37 simultaneously with injection in TSF-05. The results of this simulation indicate that the COD distribution caused by the hypothetical injection well is much larger in area than that resulting from TSF-05 injection alone. While aquifer properties in some areas are uncertain, the semi-quantitative assessment of the relative value of injecting at two separate wells rather than at a single injection well is considered valid.

4.3.3 Conclusions and Recommendations

Overall, the model is a useful tool for evaluating potential electron donor injection scenarios. However, better characterization of transport properties (including COD sorption and decay rates) and aquifer properties (including unidentified local scale heterogeneities) will improve the effectiveness of the model for this purpose. Also, it is important to the reliability of the model to obtain sufficient data to construct reasonable observed COD breakthrough curves at TAN-25 and TAN-31, and perhaps at TSF-05. This information is needed to limit the range of key model parameters, including hydraulic conductivity, effective porosity, COD sorption in the vicinity of TSF-05, and COD decay rates. It was determined that co-injection of sodium lactate and a conservative tracer would provide the data needed to determine these parameters. The data to improve this model was obtained from the 2002 Tracer Test.

4.4 Tracer Test Results

As described in Section 3.5, a tracer test was performed based upon recommendations to improve the TAN ISB performance model by providing more sufficient data to better characterize transport properties in the hot spot area of the aquifer (INEEL 2002d). The specific objectives of the tracer test were to:

1. Determine the porosity in the vicinity of TSF-05 relative to results from the pre-bioremediation tracer test conducted in 1998 (Wymore, Bukowski, and Sorenson 2000)

2. Determine the porosity near the edge of the residual area

3. Determine the retardation factor for the electron donor solution

4. Determine the first-order degradation rate of the electron donor measured as COD

5. Determine the actual lactate and lactate by-product fermentation rates.

The following sections present the results of the tracer test in the following areas: porosity estimate in the vicinity of TSF-05 (Section 4.4.1), porosity estimate near the edge of the source (Section 4.4.2), retardation factor for the electron donor (Section 4.4.3), electron donor degradation rate (Section 4.4.4), lactate and lactate by-product degradation rates (Section 4.4.5), and QA/QC (Section 4.4.6).

4.4.1 Porosity Estimation in the Vicinity of TSF-05

Breakthrough of the bromide and iodide tracers was observed at two sampling locations: TAN-25 (located 25 ft from TSF-05) and TAN-31 (located 50 ft from TSF-05), as shown in Figure 4-43. Neither bromide nor iodide was observed in samples from Well TAN-26 (located 50 ft from TSF-05), which is sampled approximately 27 m (90 ft) below the bottom of injection well TSF-05.

The bromide and iodide breakthrough curves were analyzed quantitatively with the same two simple models that were used to estimate aquifer properties from the 1998 Tracer Test in the immediate vicinity of TSF-05. The first model is based on the Ogata and Banks (1961) solution to the one-dimensional advection-dispersion equation for a continuous solute source. A slight modification was made to the solution to allow for a pulsed source rather than a continuous source. The pulse was modeled by subtracting the contribution of a second continuous source that was "turned on" at time t_p, where t_p is equal to the pulse duration. The concentration contributed by the second source was then subtracted from the concentration contributed by the initial source to obtain the actual solute concentration. A similar approach for modeling a recirculating tracer test can be found in the *Two-Well Tracer Test in Fractured Crystalline Rock* (Webster, Proctor, and Marine 1970). The resulting model for a one dimensional, finite pulse is:

$$C(x,t) = \left(\frac{C_0}{2}\right) erfc\left[\frac{x - vt}{2(\alpha_x vt)^{0.5}}\right] - \left(\frac{C_0}{2}\right) erfc\left[\frac{x - vt_p}{2(\alpha_x vt_p)^{0.5}}\right] \quad (4\text{-}12)$$

where

C = the tracer concentration

x = distance from the injection well

t = time since tracer injection

C_0 = the tracer injection concentration

v = the average groundwater velocity (retardation of the tracer is assumed to be insignificant)

α_x = the longitudinal dispersivity.

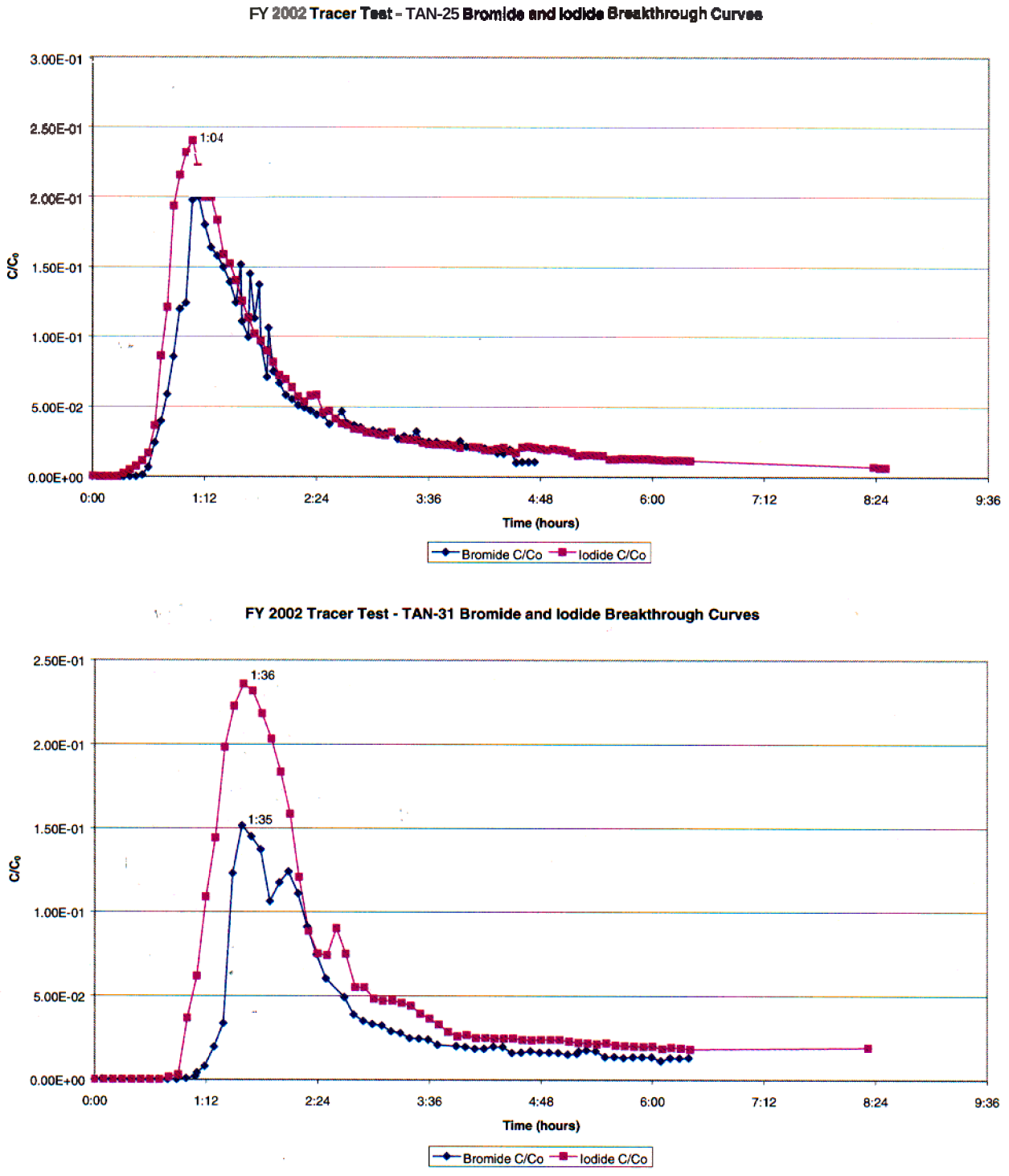

Figure 4-43. Bromide and iodide breakthrough curves for *TAN-25* and TAN-31.

Aquifer properties were estimated by fitting the model to the observed bromide and iodide breakthrough curves. The fitting parameters were C_0, v, and a_x. While the concentration of tracer in the tracer solution before injection was known, it is not equal to C_0, which is the tracer concentration in groundwater immediately outside the injection well, because of dilution in the well and in the gravel pack around the well. Rather than trying to estimate the effect of this dilution, C_0 was used as a fitting parameter. Ideally, C_0 would be the same for all breakthrough curves. The average velocity was converted to effective porosity using the relationship that the average velocity is equal to the volumetric flow rate divided by the average cross-sectional area for flow. The observed and modeled bromide and iodide breakthrough curves for TAN-25 and TAN-31 are shown in Figure 4-44; the parameters providing fits are given in Table 4-18.

Table 4-18. Transport properties based on modified Ogata-Banks (1961) analysis of 2002 Tracer Test Data.

Well	Tracer	Distance from TSF-05 (ft)	C_0 (mg/L)	v (ft/min)	α_x (ft)	1998 Effective Porosity	2002 Effective Porosity (%)
TAN-25	Bromide	25	4,100	0.38	1.6	0.1	0.09
TAN-25	Iodide	25	8,700	0.37	2.2	NA	0.2
TAN-31	Bromide	50	3,300	0.5	1.5	0.05	0.03
TAN-31	Iodide	50	10.000	0.51	2.5	NA	0.06

While the fits of the model to the observed breakthrough curves (as shown in Figure 4-44) are not perfect, they are reasonably close considering a simple one-dimensional model was used for a complex, heterogeneous, three-dimensional system. The differences are attributed to the differences in the flow paths from the injection well to the various observation wells. The different flow paths probably vary in the extent to which they violate the assumption of one-dimensionality. Nonuniform mixing in and immediately around the wellbore probably contributed as well.

Since the flow rate for the sodium lactate and the potable water during this injection was approximately twice the flow rate of potable water during the injection of bromide tracer (140 L/min versus 76 L/min [38 gpm versus 20 gpm]), but the peak breakthrough times were similar, the Ogata-Banks model estimates different porosity values from both tracers. For both TAN-25 and TAN-31, effective porosity estimated from the bromide tracer is similar to the estimate obtained using the 1998 Tracer Test data; yet, the effective porosity estimated using the iodide, which was injected with sodium lactate, is approximately twice that using bromide for TAN-25 (Table 4-18). Using this data and the Ogata-Banks model, it is difficult to determine if the porosity has increased between TSF-05 and TAN-25 and TAN-31 during the period between the 1998 and 2002 Tracer Tests.

The second model applied to the tracer test data, the "bull's eye" model (Wymore, Bukowski, and Sorenson 2000), estimated the average effective porosity between the observation wells and the injection point using the distance between the wells, the time to peak tracer arrival, and the volume of water injected. Results using this model are shown in Table 4-19. The volume of water injected is the injected flow rate multiplied by the time to peak tracer arrival. The bulk volume is the total volume calculated for a cylinder with a radius equal to the distance between wells and a height equal to the injection interval thickness (30 m for TSF-05). This analysis assumed radial flow from the injection well. The effective porosity was then calculated using the volume of water that had to be injected to drive the tracer to the observation well divided by the bulk volume.

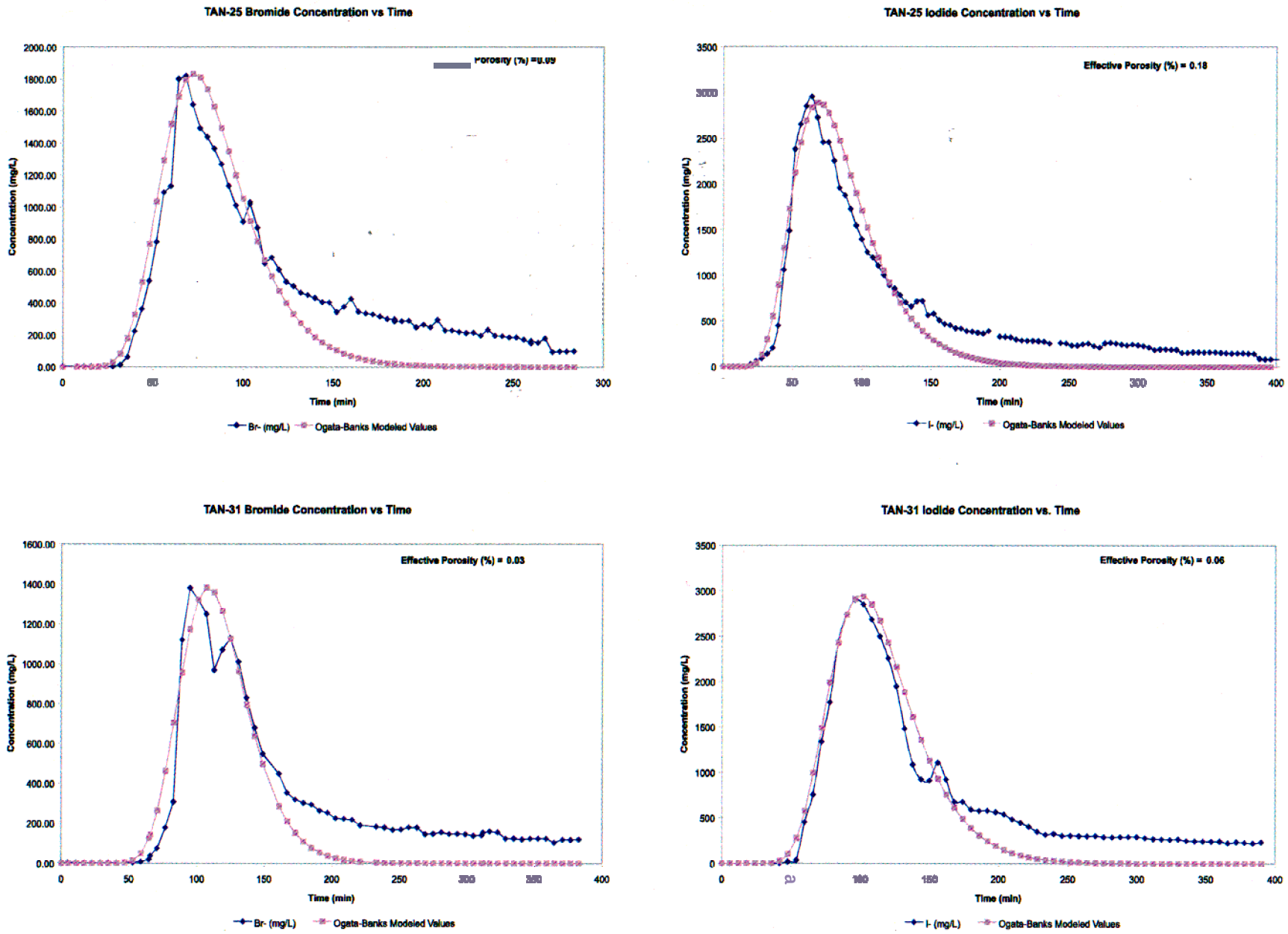

Figure 4-44. Bromide and iodide breakthrough curves and analytical model calibration results for TAN-25 and TAN-31.

Table 4-19. Calculation of effective porosity from 2002 Tracer Test data using bull's eye model.

Well	Tracer	Distance from TSF-05 (m)	Time to Peak (min)	Volume Injected (L)	Bulk Volume (10^6 L)	1998 Effective Porosity	2002 Effective Porosity
TAN-25	Bromide	7.6	68	5,440	5.44	0.06%	0.1%
TAN-25	Iodide	7.6	64	8,975	5.44	NA	0.2%
TAN-31	Bromide	15	95	7,483	21.2	0.04%	0.04%
TAN-31	Iodide	15	96	13,337	21.2	NA	0.06%

The bull's eye model, using distance and time of peak arrival, resulted in estimating porosity values that were similar to those estimated by Ogata-Banks. Like the Ogata-Banks estimates, effective porosity for both TAN-25 and TAN-31 are similar to the 1998 Tracer Test results for bromide; however, the value estimated using iodide is approximately twice that of bromide (Table 4-19). Once more, given that the properties of the sodium lactate electron donor solution appear to slow fluid transport relative to a conservative tracer in water only, and that the heterogeneous and complex flow paths violate the assumption of radial flow, it is difficult to determine if porosity has increased between TSF-05 and TAN-31 during the period between the 1998 and 2002 Tracer Tests using the bull's eye model. However, the bull's eye model does appear to indicate that effective porosity has increased between TSF-05 and TAN-25 based on the bromide tracer data.

4.4.2 Porosity Estimation Near the Edge of the Residual Area

The porosity near the edge of the residual source area was to be estimated using iodide concentrations measured from samples collected at wells TAN-D2 (located 115 ft from TSF-05), TAN-26 (located 50 ft from TSF-05), TAN-37A (pump at 240 ft below land surface [bls]), TAN-37B (pump at 275 ft bls), and TAN-37C (pump at 379 ft bls); TAN-37 is located 148 ft from TSF-05. No increasing iodide concentration trends or breakthrough were observed at TAN-26, TAN-37A, TAN-37B, or TAN-37C during the tracer test period. Breakthrough of iodide at TAN-D2 was observed and is shown in Figure 4-45.

Iodide breakthrough was analyzed quantitatively using the same two models, Ogata-Banks and the bull's eye model, as described above in Section 4.4.1. The fit of the Ogata-Banks model to the observed breakthrough curve is shown in Figure 4-46, and the parameters providing the fit are shown in Table 4-20.

Table 4-20. Transport properties based on modified Ogata-Banks (1961) analysis of 2002 Tracer Test Data.

Well	Tracer	Distance from TSF-05 (ft)	C_0 (mg/L)	v (ft/min)	a, (ft)	1998 Effective Porosity	2002 Effective Porosity
TAN-D2	Bromide	115	4,000	0.015	25	0.4%	NA
TAN-D2	Iodide	115	2.000	0.027	25	NA	0.5%

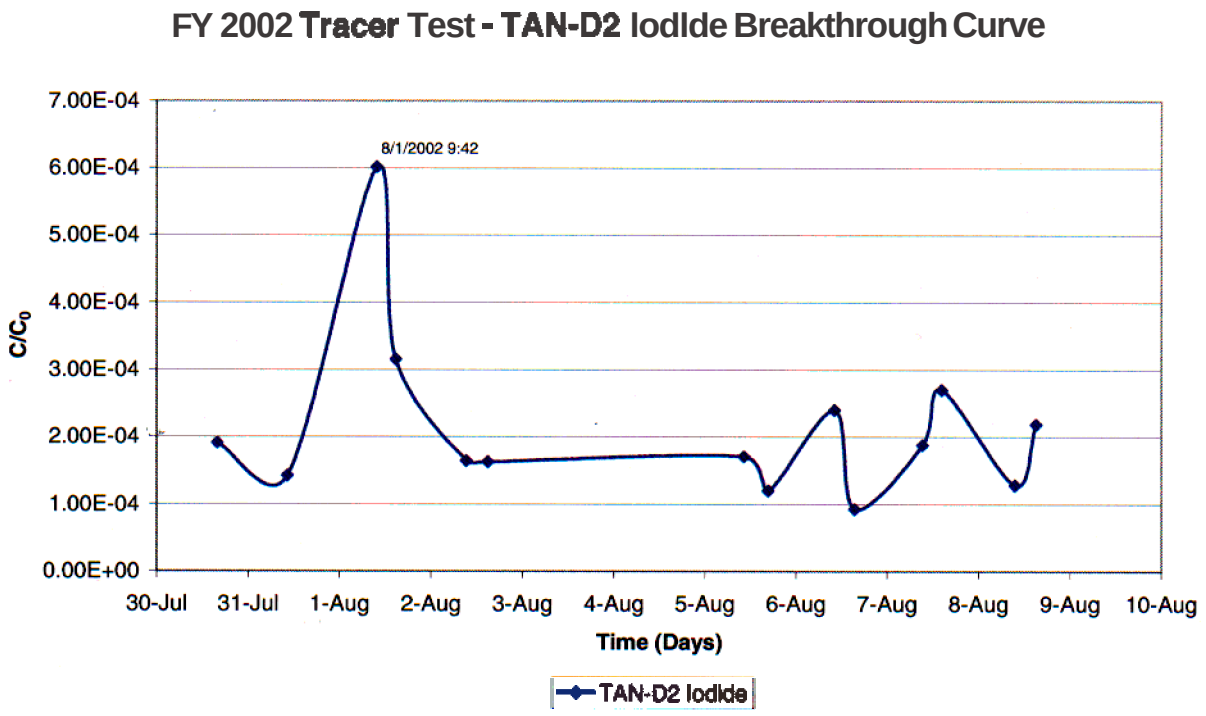

Figure 4-45. Iodide breakthrough *curve* for TAN-D2.

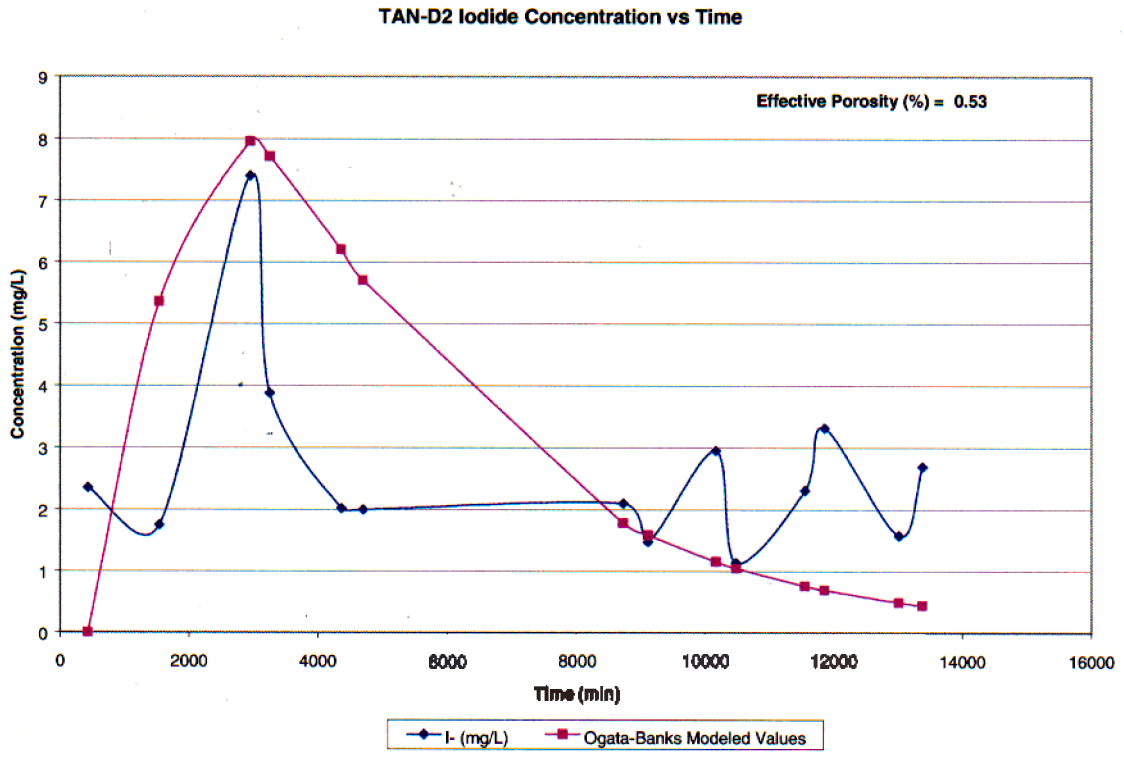

Figure 4-46. Iodide **breakthrough curve** and **analytical model calibration result** for TAN-D2.

The fit of the model to the observed breakthrough curve for TAN-D2 (as shown in Figure 4-46) was not as close as for wells TAN-25 and TAN-31 (Figure 4-44). The difference may be attributable to more heterogeneous and complex flow paths between TSF-05 and TAN-D2 compared with the closer wells (TAN-25 and TAN-31). This is probably due to TAN-D2 being located upgradient of TSF-05 and less frequent sampling at TAN-D2 during the tracer test resulting in a less precise breakthrough curve. The complex flow paths and nonuniform mixing of the tracer solution as it moved through the aquifer probably contributed as well. The fitting parameters for the velocity and the dispersivity are each approximately one order of magnitude different for TAN-D2 (Table 4-20) than for TAN-25 and TAN-31 (Table 4-18 and 4-19). These data suggest that, similar to the results from the 1998 Tracer Test, the effective porosity is lower near TSF-05 relative to the larger scale and the dispersion is smaller because of limited flow paths near the injection well.

The bull's eye model applied to the tracer test estimated the average effective porosity between the observation well and the injection point using the distance between the wells, the time to peak tracer arrival, and the volume of water injected (as discussed previously in Section 4.4.1). Results are shown in Table 4-21. The bull's eye model, using distance and time of peak arrival, resulted in estimating porosity values that were slightly less than those estimated by Ogata-Banks. Like the Ogata-Banks estimates, effective porosity was similar to the 1998 Tracer Test results that used bromide (Table 4-21). Estimates from both the Ogata-Banks and bull's eye model seem to indicate that there has been no change in porosity between TSF-05 and TAN-D2 during the period between the 1998 and 2002 Tracer Tests.

Table 4-21. Calculation of effective porosity for TAN-D2 using bull's eye model.

Well	Tracer	Distance from TSF-05 (m)	Time to Peak (min)	**Volume Injected (L)**	Bulk Volume (10^6 L)	1998 Effective Porosity	2002 Effective Porosity
TAN-D2	Bromide	35	5409	368,600	117	0.3%	NA
TAN-D2	Iodide	35	2946	401,792	117	NA	0.3%

4.4.3 Retardation of Electron Donor

Data were collected during the 2002 Tracer Test to estimate the retardation factor of electron donor (i.e., the relative transport rate of lactate compared to that of water) to improve the numerical modeling of electron donor injection strategies. The retardation factor is the empirical parameter commonly used in transport models to describe the chemical interaction between a compound and geological materials. The retardation factor accounts for processes such as surface adsorption, absorption into the soil or sludge structure, and precipitation. The improved model data would then be used in simulations designed to optimize the bioavailability of lactate in the source area. The retardation factor, R_f, is defined as:

$$R_f = \frac{V_p}{V_c} \tag{4-10}$$

where

V_p = velocity of water (represented by the tracer solution)

V_c = velocity of compound (sodium lactate in this case).

The distribution coefficient, K_d, can also be calculated by from the R_f using the following relationship:

$$R_f = 1 + \frac{\rho_b}{\eta_e} K_d \qquad (4\text{-}11)$$

where

ρ_b = porous media bulk density

η_e = effective porosity of the media at saturation.

Equation 4-11 assumes that all reactions go to equilibrium and are reversible and that the chemical environment along the solute flow path does not vary with either space or time (EPA 1999).

Samples that had been collected every 4 minutes at TAN-25 and every ***6*** minutes at TAN-31 were analyzed for concentrations of iodide tracer and COD to determine the retardation factor of the sodium lactate solution. The TAN-25 and TAN-31 breakthrough curves for iodide and COD are shown in Figure 4-47. **As** can be seen in Figure 4-47, the iodide shows a clear breakthrough curve while the sodium lactate increases and remains elevated. This is because the iodide solution injection was completed within 22 minutes, while the injection of the sodium lactate solution continued for approximately 22 hours after the iodide tracer injection was completed (sodium lactate was injected during a routine 4X 3% injection, see Section 3.5). Therefore, the data do not produce a breakthrough curve that supports an accurate calculation of the velocity of sodium lactate. Due to the lack of a quantitative velocity for the sodium lactate, Equation 4-10 could not be used to calculate a quantitative retardation factor for the sodium lactate. However, by noting the similarities between the front side of the curves that represent the velocity of water (iodide tracer) and the velocity of the sodium lactate, it can be qualitatively stated that the retardation of sodium lactate is approximately equal to that of iodide. In other words, no significant retardation of sodium lactate was observed along the flow paths from TSF-05 to TAN-25 and TAN-31 during this test.

4.4.4 Electron Donor Degradation Rate

In additibn to the retardation factor, the other key parameter needed for the ISB performance model to simulate transport of electron donor is the first-order decay rate constant. COD decay rates initially used in the ISB model were calculated from COD concentrations measured during the PDP-I phase; however, these values were deemed to be too low between TSF-05 and TAN-25 and TAN-31 in order to support a reliable simulati'on by the model. In order to reliably simulate the precise distribution of COD near the injection well, it was recommended that the COD decay rates be determined by co-injecting sodium lactate and a conservative tracer (INEEL 2002d).

First-order decay calculations were performed for electron donor utilization using electron donor as (1) sodium lactate, (2) the sum of sodium lactate, acetate, and propionate, and (3) COD for wells TAN-25 and TAN-31. In addition, this analysis assumed that the quantity being experimentally monitored (electron donor) versus time was linearly related to the concentration of the exponentially decaying total electron donor. The method and equations used to determine the first-order decay rates are found in Section 4.1.1.2. The degradation rates presented here differ from those presented in Section 4.1.1.2 because these were based on the relative continuous data collected during the tracer test, while the rates presented in Section 4.1.1.2 were based on ISB operational data that essentially consisted of two data points after each sodium lactate injection. A comparison of the rate constants calculated from both datasets (i.e., the tracer test and ISB operational data) is presented in Section 5.2.2.

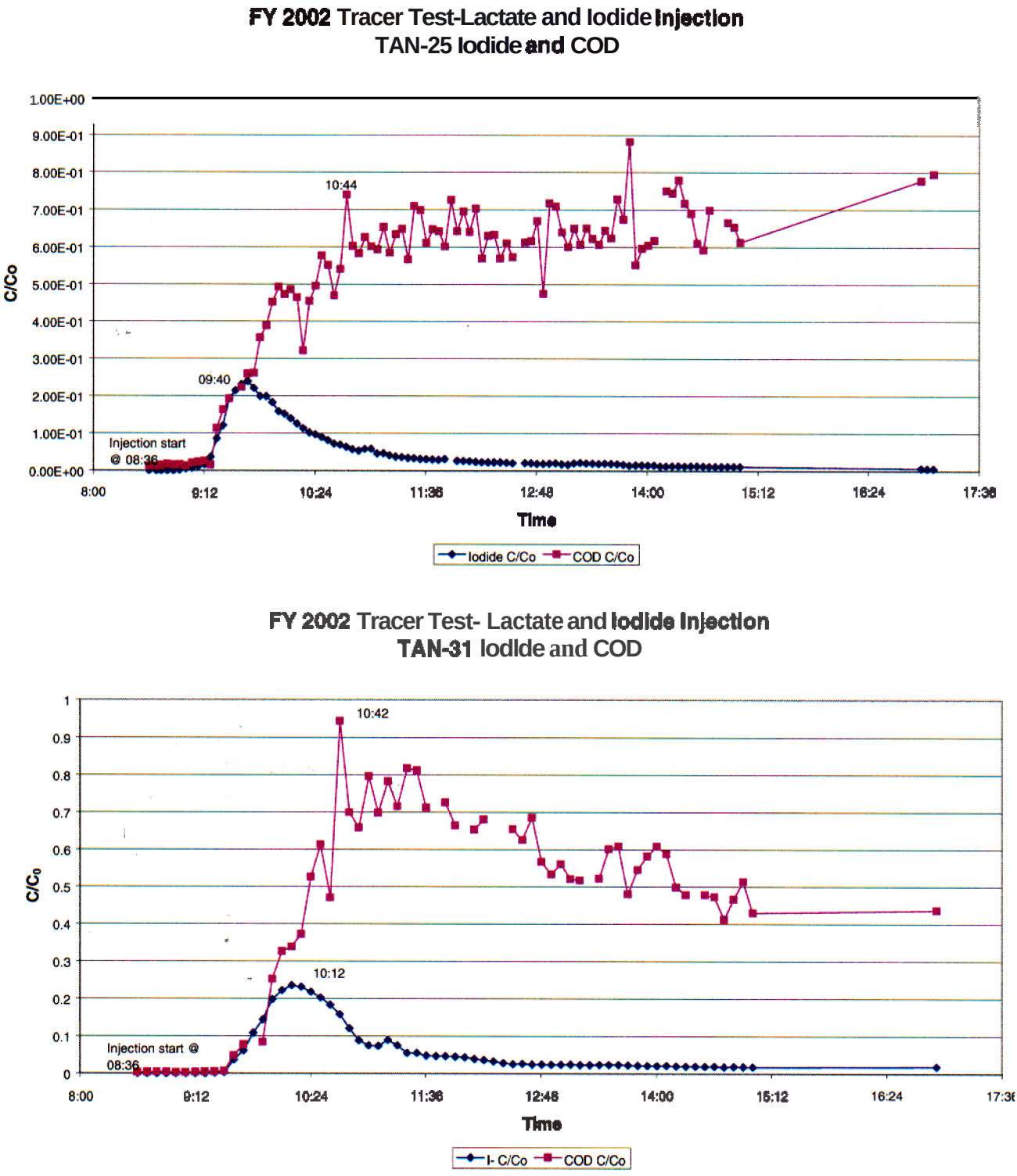

Figure 4-47. TAN-25 and TAN-31 breakthrough curves for iodide and chemical oxygen demand.

The degradation of COD and sodium lactate over time in wells TAN-25 and TAN-31 are presented in Figures 4-48 and 4-49. Using the data from these figures and Equation 4-7, a "straight line" plot with the slope equal to "-*k*" is produced. Figures 4-50 and 4-51 show these plots. The same technique was used to calculate the total VFA degradation rate constant (Figure 4-52). The first order rate constants for the COD, sodium lactate, and total VFAs for source wells TAN-25 and TAN-31 from the 2002 Tracer Test are listed in Table 4-22.

As shown in Table 4-22, sodium lactate had the highest rate constant compared to the total VFAs and COD. This is expected as sodium lactate is degraded relatively rapidly compared to propionate and acetate, which represent a significant fraction of the total VFAs and COD. Also, TAN-31 had higher rate constants than TAN-25. This shows that VFAs and COD disappear faster once they get to TAN-31. From Figures 4-49, 4-50, and 4-51, close to the same concentration of COD, VFAs, and sodium lactate arrived at TAN-31 and TAN-25, but it was utilized faster in TAN-31. This probably is not a function of distance, but of the greater impact of aerobic injection solution on TAN-25 compared to TAN-31 (see discussion in Section 4.1.1.2).

4.4.5 Sodium lactate and Sodium lactate By-product Fermentation Rates

Table 4-22 lists the first order rate constants calculated for sodium lactate, COD, and total VFAs during the 2002 tracer study. As described above, the VFA rate constant correlates well with the COD rate constant (0.15 and 0.18 for TAN-25), whereas the lactate rate constant is higher by a factor of two (0.33 from TAN-25). Based on these results, COD appears to be a good indicator for total electron donor. For purposes of modeling the actual lactate distribution, however, lactate is degraded much faster than COD and therefore using the lactate rate constant would be more appropriate. These differences can be attributed to the relatively slow degradation of lactate fermentation products propionate and acetate within the system. This is supported by field data, which show that lactate was generally rapidly utilized and propionate and acetate accumulated before they were slowly degraded.

It was not possible to calculate a propionate or acetate degradation rate with the available data. The degradation of propionate and acetate is not energetically favorable in the presence of lactate. Therefore, significant propionate degradation does not occur until the lactate is mostly utilized. The duration of sampling was not sufficient to collect adequate data to document the complete utilization of lactate and the onset of propionate degradation. Therefore, it was not possible to calculate a propionate or acetate fermentation rate. A more focused data collection effort, with samples collected on a more frequent basis and over a longer duration, would be required in order to perform this calculation.

4.4.6 Quality Assurance/Quality Control

Precision and accuracy for the 2002 Tracer Test was evaluated through performance of duplicates and standards. The completeness goal for the 2002 Tracer Test was 90% for bromide, iodide, and COD samples, with duplicates being collected at a frequency of one every twenty samples (5%). The complete 2002 Tracer Test QA results are reported in Appendix F.

Precision was evaluated through collection of duplicate samples. The W D was calculated for duplicate samples, with a target W D of 10% for bromide and iodide samples, 50% for COD samples less than or equal to 125 mg/L, and 25% for COD samples greater than 125 mg/L. The W D values for bromide and iodide duplicates were within the target 10% for all analyses except for three bromide and two iodide duplicates. All but three of the COD duplicates had RPDs within the acceptable range.

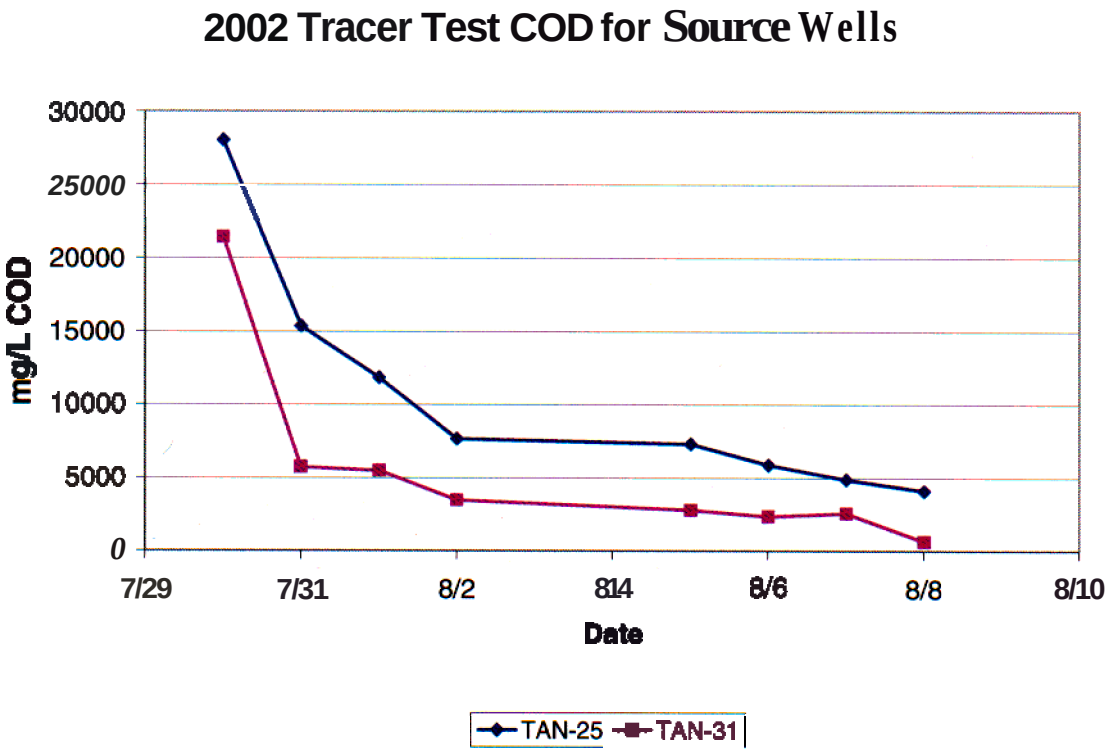

Figure 4-48. Degradation of chemical oxygen demand in TAN-25 and TAN-31.

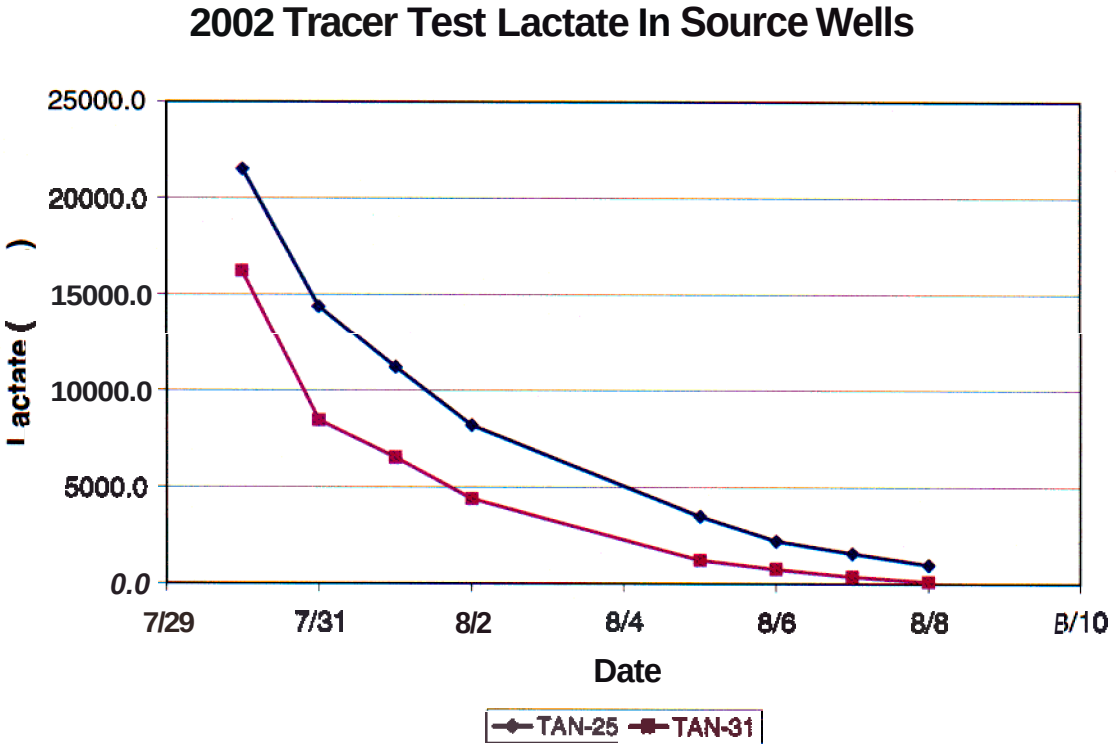

Figure 4-49. Degradation of sodium lactate over time at wells TAN-25 and TAN-31.

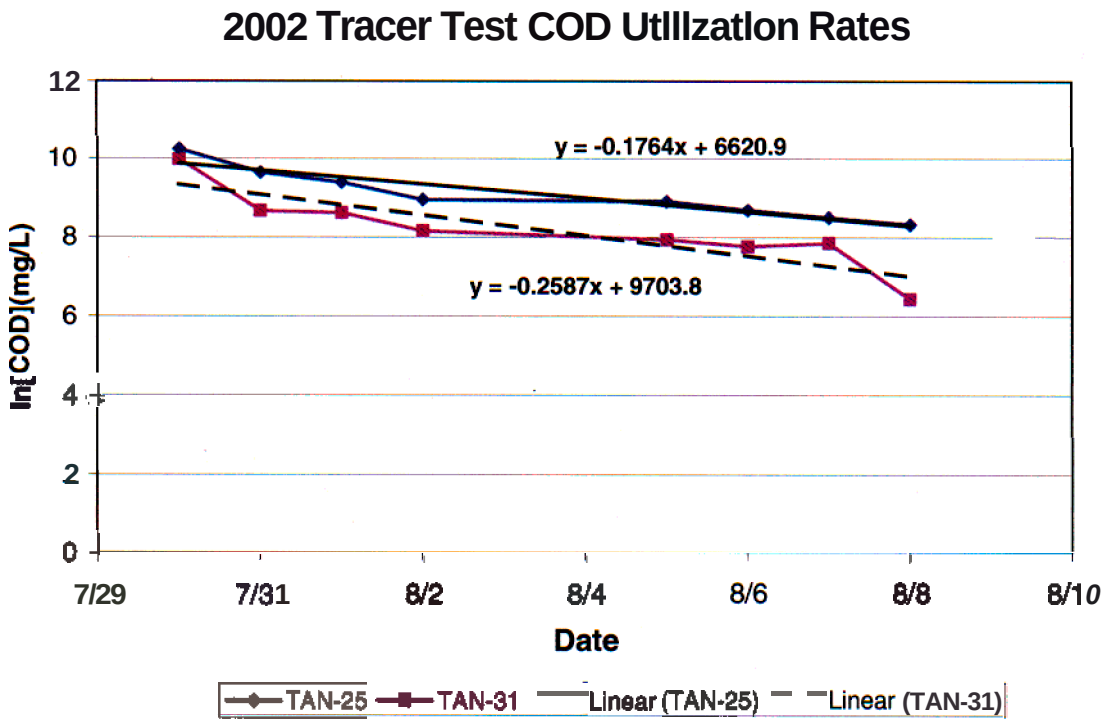

Figure 4-50. Natural log chemical oxygen demand values versus time.

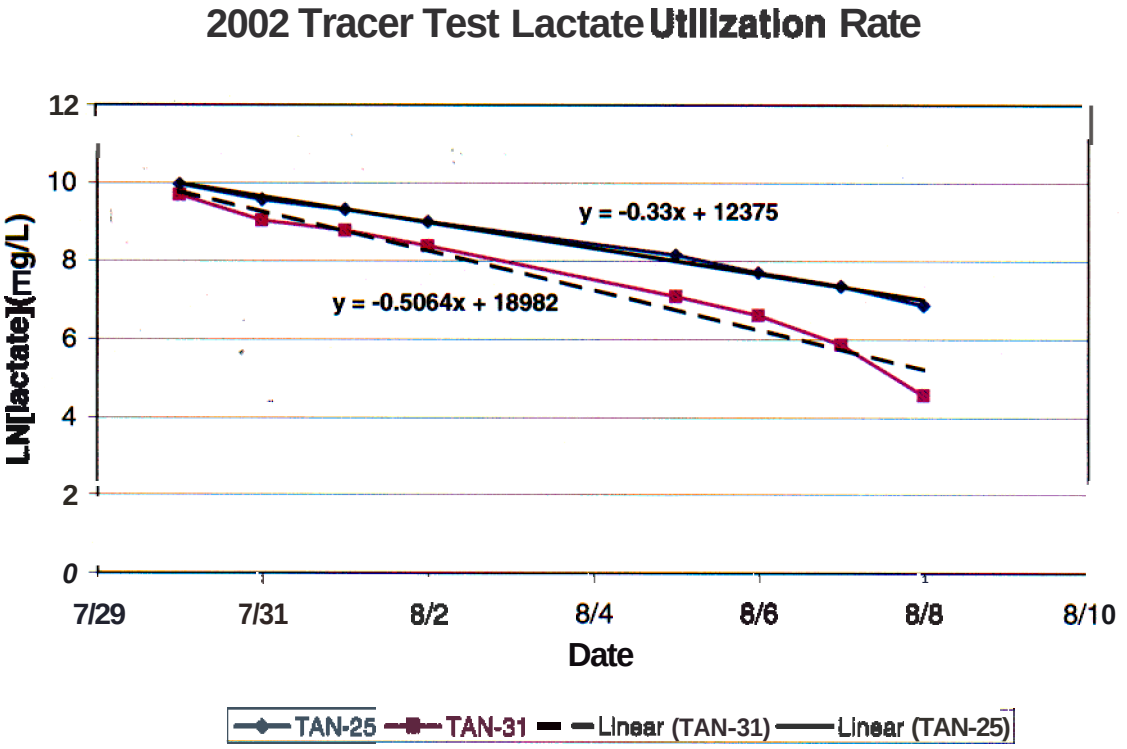

Figure 4-51. Natural log sodium lactate values versus time.

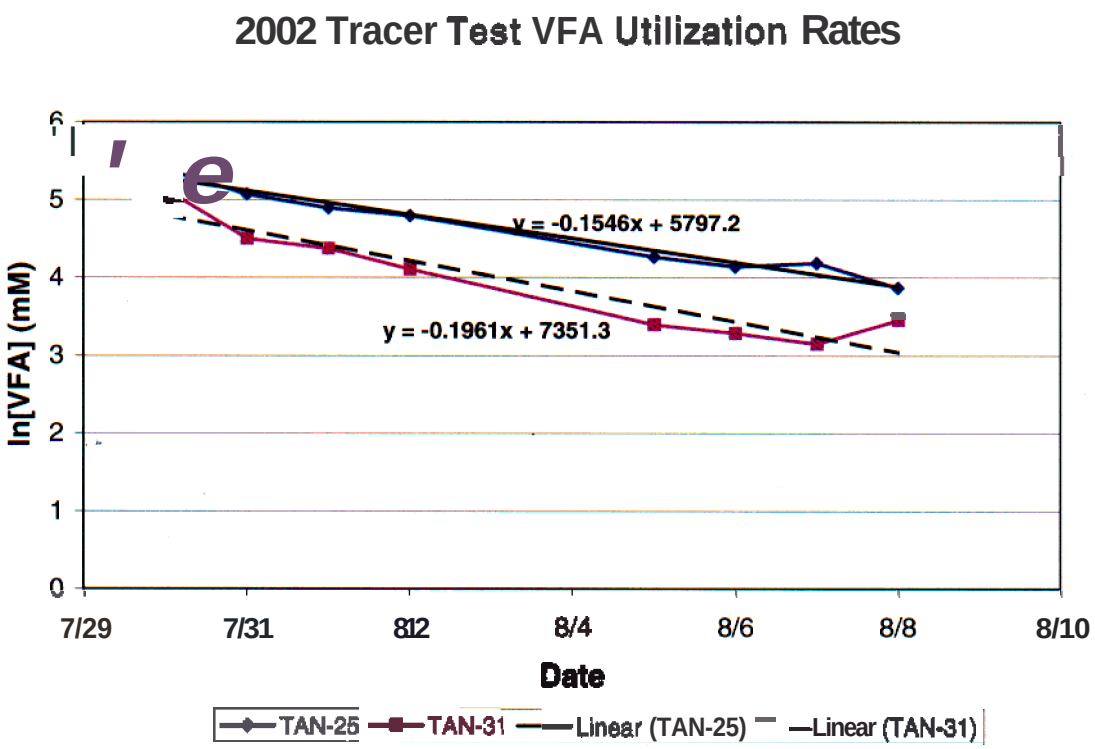

Figure 4-52. Natural log volatile fatty acid values versus time.

Table 4-22. First-order degradation rates for the source wells during 2002 Tracer Test.

	First-Order Rate Constant – k (1/day)		
Well	Sodium lactate	Total VFA	COD
TAN-25	0.33	0.15	0.18
TAN-31	0.51	0.20	0.26

Accuracy was evaluated through performance of standards. Standards were performed at least Once per 20 samples. All standards for COD were within the 90% - 100% recovery limits. Bromide and iodide standards were performed at a frequency of at least 1 per 20 samples. If the reading was more than 10% from the accepted standard concentration, the electrode was standardized according to the manufacturer's instructions.

4.5 Alternate Electron Donor Laboratory Studies Results

As described in Section 3.6, laboratory studies were performed to evaluate the potential effectiveness of several AEDs. These studies were composed of four parts, the results of which are presented in the following sections: *ARD* Efficiency (Section 4.5.1), IFT Analysis (Section 4.5.2), Molecular Analysis (Section 4.5.3), and Metals Analysis (Section 4.5.4).

4.5.1 Anaerobic Reductive Dechlorination Efficiency

As described in Section 3.6, the objective of this activity was to compare the dechlorinating efficiency of cultures derived from TAN using various AEDs to that of cultures using sodium lactate.

This section summarizes the results obtained from this study. A complete presentation of the results can be found in the Fiscal Year 2002 Alternate Electron Donor Evaluation (INEEL 2003a).

The ability to develop a TCE-dechlorinating laboratory culture proved somewhat difficult. Out of four bioreactors inoculated with TAN-25 groundwater, TCE, and sodium lactate, only one performed efficient ARD of TCE to ethene after a period of 1 year. Significant parent compound (TCE) was observed in all the other cultures, indicating a lack of significant dechlorinating activity. Therefore, the single culture that exhibited efficient ARD was used to inoculate cultures for the AED evaluation.

The ARD studies were performed over a 14-month period. Five flasks were inoculated with the dechlorinating culture and amended with TCE (PCE was added instead of TCE on one occasion) and one of the four AEDs (sodium lactate, cheese whey, and feed-grade and food-grade molasses [the fifth was a killed control]). Eleven months after inoculation, ARD of all amended TCE to ethene was observed in all of the AED cultures. Over the next 5 months, a detailed analysis was performed to track all amended electron donor, TCE, PCE, and the ARD products to assess the differences between electron donor utilization and ARD efficiency between the various AEDs/cultures.

Anaerobic reductive dechlorination efficiency of the cultures was assessed based on the degradation of parent compounds (PCE and TCE) and the accumulation of ARD daughter products. Specifically, ethene accumulation (on a molar basis) was used as the success criteria for the cultures and the focus of the cost-benefit analysis. The most efficient ARD occurred within the sodium lactate culture, which had no cis-DCE, very little VC accumulation, and the highest ethene concentrations at the end of the study. Ethene accounted for approximately 92% of the amended TCE/PCE (molar basis). Food-grade molasses and cheese whey both had low cis-DCE accumulation, some VC accumulation (food-grade molasses was much higher), and very similar ethene production. In these cultures, ethene represented approximately 56 and 44% of the original TCE/PCE. Feed-grade molasses was the only culture with significant PCE, TCE, and cis-DCE accumulation and had the lowest ethene production. In this culture, ethene represented only 25% of the original TCE/PCE.

Anaerobic reductive dechlorination efficiency was also assessed using the TCE degradation rate from ethene generated for the AED cultures during the latter part of the study. The degradation rate incorporated both the TCE and PCE additions to the cultures. Degradation of all parent compound occurred in all of the AED cultures except feed-grade molasses. The sodium lactate culture had the highest degradation rate (6.9 μg/d), followed by the food-grade molasses (4.16 μg/d), cheese whey (3.34 μg/d), and lastly the feed-grade molasses cultures (1.83 μg/d) (Table 4-23).

Table 4-23. Cost analysis of electron donors.

	Total COD (g)	Ethene[a] (μmol)	COD/Ethene[a] (lb/mol)	COD ($/lb)	Ethene[a] ($/mol)	TCE ($/lb)	TCE/d[b] (pg)
Sodium Lactate	0.016	4.41	8.0	1.36	10.88	37.62	6.90
Molasses (food)	0.026	2.66	21.5	0.06	1.30	4.48	4.16
Molasses (feed)	0.026	1.17	48.9	0.05	2.55	8.82	1.83
Cheese Whey	0.026	2.13	26.9	0.42	11.15	38.59	3.34

a. These values indicate the amount of ethene generated over an 84-day incubation period per microcosm.
b. These values indicate the mass of TCE dechlorinated per day, calculated from amount of ethene generated over an 84-day incubation period.

The electron donor utilization also varied between the cultures. Propionate and acetate accumulation was observed in all of the cultures. Propionate was observed at the highest concentrations in the food-grade molasses and sodium lactate cultures, and very little accumulation was observed in the cheese whey and feed-grade molasses cultures. Food-grade molasses and sodium lactate also had very high concentrations of acetate, followed by cheese-whey and feed-grade molasses.

The ARD performance was correlated with electron donor utilization to assess a relative cost benefit for each electron donor. Total ethene production and total electron donor utilization as COD were used to determine the cost per pound of TCE dechlorinated to ethene. The results of this analysis indicated that food-grade molasses was the most cost efficient electron donor in terms of cost per unit of ethene generated followed by feed-grade molasses, sodium lactate, and cheese whey. The molasses cultures performed well in the cost-effective calculation because of their relatively low cost per pound of COD ($0.05 to 0.06/lb COD) compared with sodium lactate ($1.36/lb COD.) and cheese whey ($0.42/lb) (Table 4-23). This calculation, however, only accounted for the cost per unit of TCE or PCE dechlorinated to ethene and did not account for the degradation rate. Therefore, although feed-grade molasses performed well in the cost analysis, it was the only culture that did not degrade all parent compounds within the timeframe of the study. At this point, it is unclear whether the potential cost savings of these lower-cost electron donors would be offset by a longer remedial timeframe due to lower ARD rates.

4.5.2 Interfacial Tension Analysis

As stated in Section 3.5, IFT measurements were performed for sodium lactate and several AEDs to evaluate their potential to enhance TCE bioavailability in situ. These AEDs included ethyl lactate/sodium lactate mixture, sodium dipropionate, molasses, oleolactylic acid (LactOil™), whey powder, unground lactose, ground lactose, purified dairy carbohydrate, and unpurified dairy carbohydrate. A summary of the results is presented here.

The results of the IFT studies illustrated significant decreases (> 10%) in IFT for high sodium lactate concentrations (>30% solution). These data show that sodium lactate by itself had a significant effect on IFT at higher concentrations, which supported the field data and the bioavailability enhancement hypothesis. The IFTs of the sodium lactate and ethyl lactate mixtures were a hnction of ethyl lactate concentration and not of sodium lactate concentration. Therefore, higher concentrations of ethyl lactate resulted in the stepwise decrease of IFT, regardless of sodium lactate concentration. These data indicate that the presence of ethyl lactate significantly decreased IFT at even relatively low sodium lactate concentrations. Because of this, these AEDs will not be studied further at this time.

Sodium dipropionate, molasses, and LactOil™ had significantly lower IFTs at all concentrations than did sodium lactate. The IFT properties of five different whey products (whey powder, unground lactose, ground lactose, purified dairy product, and unpurified dairy product) showed that only two of the five whey products—whey powder and unpurified dairy product—achieved substantial IFT reductions. IFT values for ground lactose, unground lactose, and purified dairy product did not decrease at higher concentrations. This implies that these AEDs would not have a significant bioavailability enhancement effect on pure phase TCE.

4.5.3 Molecular Analysis

As described in Section 3.5, molecular analysis was performed to characterize microbial community changes under the conditions of utilization of the various AEDs. Microbial community changes were evaluated for the food-grade molasses, feed-grade molasses, cheese whey, and sodium lactate cultures. A summary of the results is presented here, while a thorough presentation can be found in Appendix E.

Molecular microbial community characterization uses DNA extracted from samples to determine qualitative or semi-quantitative differences in the community composition over time and/or under a change in stimulus. This technique can also be used to look for a specific organism or group of organisms of interest. These methods were used here to provide a quick and relatively easy assessment of the effect of the AED on the microbial community of interest. All of the molecular methods that were used focus on the 16S rRNA gene. This gene codes for the ribonucleic acid (RNA) portion of the small subunit of the bacterial ribosome, which is used to make proteins in microbial biosynthesis. Since all bacteria make protein, all bacteria have this gene, which makes it very useful in evaluating the composition of a microbial community. Differences between microbes are inferred by differences in the deoxyribonucleic acid (DNA) base sequence as adenine, thymine, guanine, and cytosine of their 16S rDNA genes. A great deal of research has been conducted to characterize and catalogue all known *Bacteria* and *Archaea* 16S rDNA sequences into comprehensive databases. By assessing the sequence similarity between an unknown sequence and the database sequences, tentative identification of species within the community can be determined. Therefore, 16S rRNA molecular methods can be used to tentatively identify individual members of a microbial community and to assess the relative diversity and abundance of populations within that community.

Two methods were used to characterize the microbial communities within the AED cultures developed using sodium lactate, feed-grade molasses, food-grade molasses, and cheese whey. These methods included PCR, using universal and species-specific primers, and T-RFLP. PCR was performed using primers specific for DHE to assess the presence or absence of this species within the AED cultures. Amplification of DHE rDNA using PCR primers specific for these bacteria was achieved in all of the AED cultures. This analysis was conducted for detection only, and quantification of the PCR products was not performed. *Dehalococcoides ethenogenes* is considered to be an indicator species for the ability of a microbial community to completely dechlorinate TCE to ethene. Therefore, the identification of these populations during AED lab studies allows for tracking population response as it relates to enhancing ARD performance.

The number of bacterial species detected by T-RFLP for each AED culture is listed in Table 4-24. The number of shared species between the different cultures was then used to determine the species similarity, or Jaccard coefficient, between two cultures. Table 4-24 indicates the number of species detected in each of the AED cultures, the number of shared species, and the similarity between cultures as measured by the Jaccard coefficient. According to the Jaccard coefficient of similarity, the feed- and food-grade molasses cultures shared the greatest percentage of species (0.56), and cheese whey and sodium lactate cultures (0.33) were the least similar. The food-grade molasses was the most similar to the sodium lactate culture (0.45). Overall, these data suggest that all of the cultures were significantly different, with similarity values ranging from 33 to 56%.

Despite significant differences between the bacterial consortia in the AED cultures, DHE and *Dehalospirillum multivorans* were both detected within the T-RFLP profiles. These bacteria are of particular importance because they are isolated and characterized dechlorinating bacteria. According to the T-RFLP profiles, this bacterium accounted for 27% of the total population in the food-grade molasses

Table 4-24. Species similarity of cultures amended with food-grade molasses, feed-grade molasses, cheese whey, and sodium lactate.

First Community		Second Community		Combined Communities	
AED	Species Detected	AED	Species Detected	Shared Species	Jaccard Coefficient
Food-grade molasses	31	Feed-grade molasses	22	19	0.56
Food-grade molasses	31	Cheese whey	21	14	0.37
Food-grade molasses	31	Sodium lactate	40	22	0.45
Feed-grade molasses	22	Cheese whey	21	15	0.54
Feed-grade molasses	22	Sodium lactate	40	16	0.35
Cheese whey	21	Sodium lactate	40	15	0.33

culture, 29% in the feed-grade molasses culture, 8% in the cheese whey culture, and 20% in the sodium lactate culture (Figure 4-53). These data should be interpreted with caution, however, as they were generated using the PCR-amplified community and may not represent the actual relative abundances of members in the community. In general, however, DHE is under-represented by PCR analysis. The detection of this bacterium within all of the AED cultures indicates that all were capable of supporting this dechlorinating microbe.

Dehalospirillum multivorans is known to dechlorinate TCE to cis-DCE, but does not dechlorinate cis-DCE or VC. However, because it does have dechlorinating ability, it may also be important in TCE-dechlorinating systems. According to T-RFLP, however, only the food-grade molasses culture contained this T-RF in the community profile. Other potential dechlorinating bacteria detected within the AED cultures were Acetobacterium, which may be involved in the anaerobic cometabolism of PCE. These systems, however, are not well understood so the function performed by these bacteria cannot be conclusively determined.

The AED culture archaeal T-RFLP profiles were very similar (Figure 4-54). Each culture's T-RFLP detected three species of *Archaea*. Using clones generated from the archaeal clone library created for TAN-25 groundwater (Wood, Cummings, and Sorenson 2002), two of the three species were identified. T-RF 196 bp was *Methanothrix* and T-RF 335 was *Methanosarcina* and *Methanospirillum.* All of these *Archaea* were methanogens, which is not surprising given that significant methane production was observed in all of the cultures. *Methanothrix* and *Methanosarcina* genus are acetoclastic methanogens and *Methanospirillum* are hydrogenotrophic methanogens.

4.5.4 Metals Analysis

As described in Section 3.6.4, an analysis of the metals content of AEDs was required in order to determine if they were appropriate for injection into the subsurface at TAN. Appendix E provides a complete list of the results of the metals analyses for whey, sodium dipropionate, and several brands of food- and feed-grade molasses. Of the AEDs tested, none had metals content greater than 10 x the MCL, with one exception being sodium dipropionate, which had a lead concentration that was greater than 10 x the MCL value.

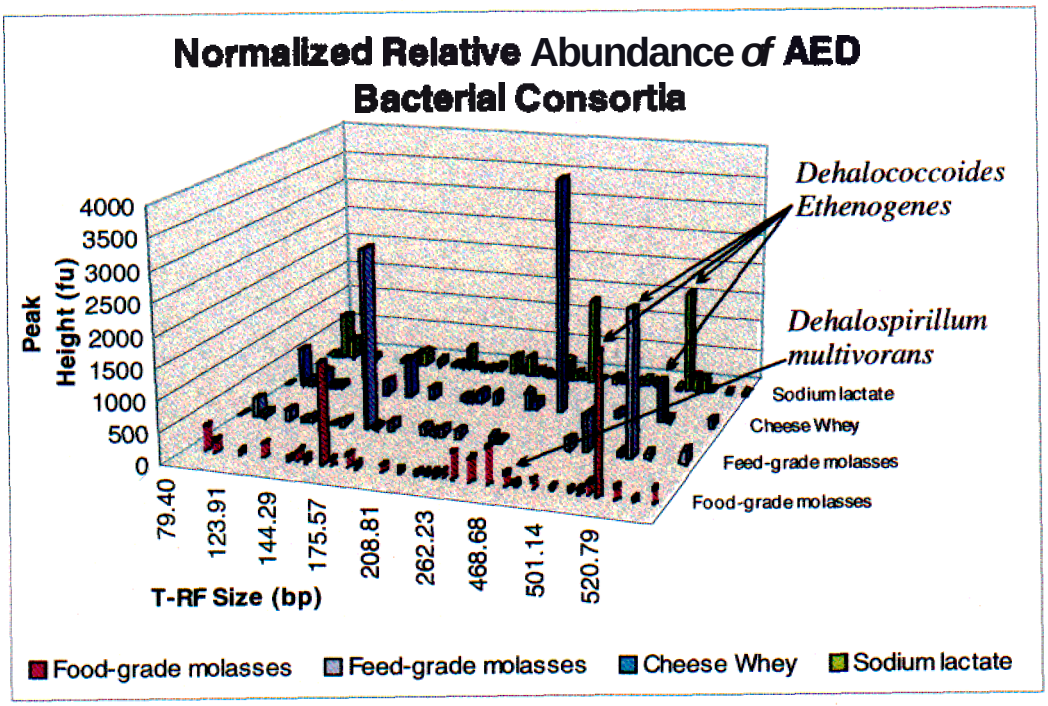

Figure 4-53, Normalized relative abundance of alternate electron donor bacterial consortia.

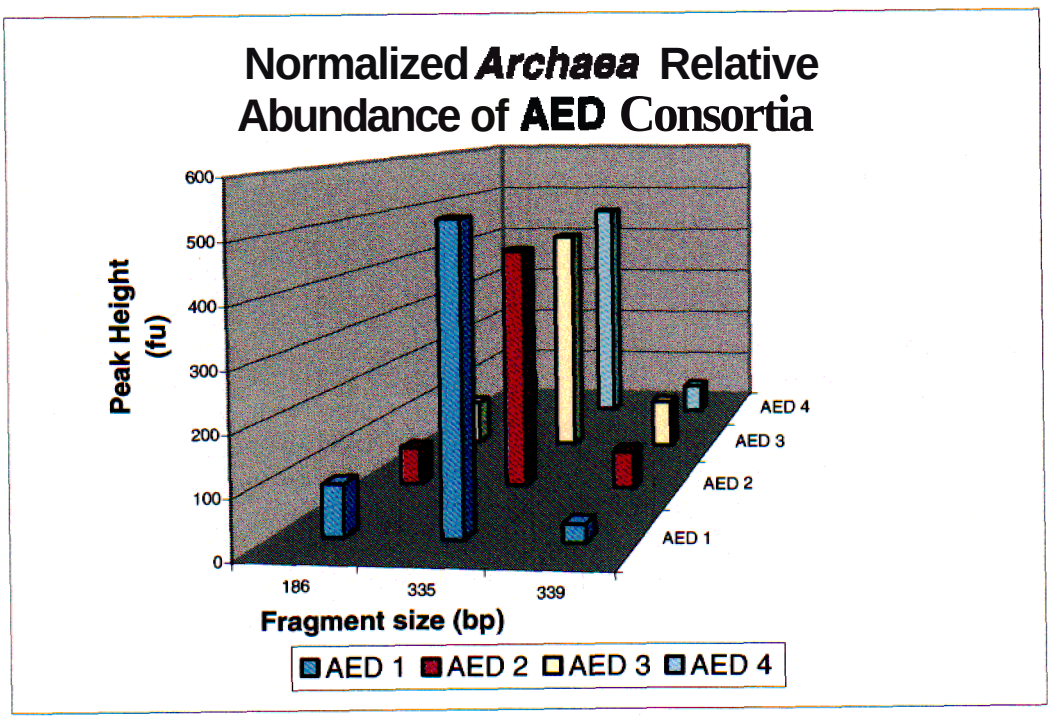

Figure 4-54. Normalized *Archaea* relative abundance of alternate electron donor consortia.